Title: Behavioral deficits, learning impairment, and enhanced hippocampal excitability in co-isogenic *Prnp*$^{ZH3/ZH3}$ mice

Authors: Matamoros-Angles, A.[1,2,3,4,#].; Hervera, A. [1,2,3,4]; Soriano, J. [5,6] ; Martí, E. [7,8] ; Carulla, P [1,2,3], Llorens, F.[3,9,10]; Nuvolone, M[11,12]. ; Aguzzi, A.[11]; Ferrer I.[3,4,13,14]; Gruart, A.[15]; Delgado-García, JM.[15,✉]; Del Río, JA. [1,2,3,4,✉]

Affiliations:

[1] Molecular and Cellular Neurobiotechnology, Institute of Bioengineering of Catalonia (IBEC), Parc Científic de Barcelona, Barcelona, Spain.
[2] Department of Cell Biology, Physiology, and Immunology, University of Barcelona, Barcelona, Spain.
[3] CIBERNED (Network Centre of Biomedical Research of Neurodegenerative Diseases), Institute of Health Carlos III, Barcelona, Spain.
[4] Institute of Neuroscience, University of Barcelona, Barcelona, Spain.
[5] Departament de Física de la Materia Condensada, University of Barcelona, Spain.
[6] Institute of Complex Systems (UBICS), University of Barcelona, Barcelona, Spain.
[7] Department of Biomedicine, University of Barcelona, Barcelona, Spain.
[8] Bioinformatics and Genomics, Center for Genomic Regulation, Barcelona, Spain.
[9] Department of Neurology, University Medical School, Göttingen, Germany.
[10] Bellvitge Biomedical Research Institute (IDIBELL), L'Hospitalet de Llobregat, Catalonia, Spain.
[11] Institute of Neuropathology, University Hospital of Zürich, Zürich, Switzerland.
[12] Amyloidosis Center, Foundation IRCCS Policlinico San Matteo, Department of Molecular Medicine, University of Pavia, Pavia, Italy.
[13] Senior Consultant, Bellvitge University Hospital, IDIBELL (Bellvitge Biomedical Research Centre), L'Hospitalet de Llobregat, Spain.
[14] Department of Pathology and Experimental Therapeutics, University of Barcelona, Barcelona, Spain.
[15] Division of Neurosciences, Pablo de Olavide University, Seville, Spain.

Current address: Institute of Neuropathology, University Medical Center Hamburg-Eppendorf, Hamburg, Germany.

Shared correspondence to:

✉ Prof. José Antonio Del Río, Institute for Bioengineering of Catalonia (IBEC), Science Park of Barcelona, the Barcelona Institute of Science and Technology, Baldiri Reixac 15-21, 08028 Barcelona, Spain.
Email: jadelrio@ibecbarcelona.eu

✉ Prof. José María Delgado-García, Division of Neurosciences, Pablo de Olavide University, 41013 Seville, Spain
Email: jmdelgar@upo.es

Abstract

The cellular prion protein (PrP^C) has been associated with numerous cellular processes, such as cell differentiation and neurotransmission. Moreover, it was recently demonstrated that some functions were misattributed to PrP^C since results were obtained from mouse models with genetic artifacts. Here we elucidate the role of PrP^C in the hippocampal circuitry and its related functions, like learning and memory, using the new strictly co-isogenic *Prnp*$^{0/0}$ mouse. Behavioral and operant conditioning tests were performed to evaluate memory and learning capabilities. *In vivo* electrophysiological recordings were carried out at CA3-CA1 synapses in living behaving mice, and spontaneous neuronal firing and network formation were monitored in primary neuronal cultures of *Prnp*$^{ZH3/ZH3}$ *vs*. wild-type mice. Results showed decreased motility, impaired operant conditioning learning, and anxiety-related behavior in *Prnp*$^{ZH3/ZH3}$ animals. PrP^C absence enhanced susceptibility to high-intensity stimulations and kainate-induced seizures. However, long-term potentiation (LTP) was not enhanced in the *Prnp*$^{ZH3/ZH}$ hippocampus. In addition, we observed a delay in neuronal maturation and network formation in *Prnp*$^{ZH3/ZH3}$ cultures. In conclusion, PrP^C mediates synaptic function and protects the synapse from excitotoxic insults. Its deletion might evoke a susceptible epileptogenic brain that would fail to perform highly cognitive-demanding tasks such as associative learning and anxiety-like behaviors.

Introduction

Cellular prion protein (PrP^C) is a cell surface GPI-anchored protein expressed in several tissues with high levels in the nervous system (Ford *et al.*, 2002; Su *et al.*, 2004), especially in neurons and glial cells (Adle-Biassette *et al.*, 2006; Bribian *et al.*, 2012; Lima *et al.*, 2007; Moser *et al.*, 1995). PrP^C is known for its crucial role in the pathogenesis of human and animal prionopathies (Aguzzi, 2000; Baldwin and Correll, 2019; Prusiner and DeArmond, 1994). In these diseases, PrP^C is transformed into a misfolded β-sheet-rich isoform, the infectious prion protein (PrP^{Sc}) (Prusiner and DeArmond, 1994). Increasing knowledge about the participation of PrP^C in prion pathogenesis contrasts with puzzling data regarding its natural physiological role (Griffoni *et al.*, 2003; Legname, 2017; Linden *et al.*, 2008; Watts *et al.*, 2018; Wulf *et al.*, 2017). Indeed, this controversy was also strengthened by the absence, until a few years ago, of an appropriate knock-out mouse model with high breeding capability to dissect biological relevance in specific processes (i.e., (del Rio and Gavin, 2016; Onodera *et al.*, 2014; Steele *et al.*, 2007; Watts *et al.*, 2018; Wulf *et al.*, 2017)).

PrP^C has been described as neuroprotective, mainly by using loss-of-function approaches (Carulla *et al.*, 2015; Chiarini *et al.*, 2002; Gavin *et al.*, 2020; Resenberger *et al.*, 2011; Roucou *et al.*, 2004), while in other studies, PrP^C overexpression was associated with increased susceptibility to neurotoxicity and cell death (Gavin *et al.*, 2020; Llorens and Del Rio, 2012; Paitel *et al.*, 2003; Paitel *et al.*, 2004; Rangel *et al.*, 2009). This might mean that *Prnp* levels should be constrained to a certain level to develop their natural functions (i.e., (del Rio and Gavin, 2016; Gavin *et al.*, 2020; Nicolas *et al.*, 2009)). This balance is altered in

several injuries and neurodegenerative processes presenting changes in mRNA and protein expression (e.g., Alzheimer's disease, dementia with Lewy bodies, some tauopathies (Goetzl *et al.*, 2020; Leng *et al.*, 2020; Lidon *et al.*, 2020; Llorens *et al.*, 2013; Vergara *et al.*, 2015), human prionopathies (i.e., sCJD (Llorens *et al.*, 2013)), and multiple sclerosis (Scalabrino *et al.*, 2015). In addition, PrP^C also plays a role in amyloid seeding and spreading in some of these diseases (Del Rio *et al.*, 2018).

As indicated, numerous studies have explored the physiological roles of PrP^C *in vivo* using $Prnp^{0/0}$ mice. However, it was demonstrated that some physiological functions were unfortunately misattributed to PrP^C due to genetic artifacts generated during the production of the most commonly used knock-out model, still in use in some laboratories: the Zürich I ($Prnp^{ZH1/ZH1}$) mouse (Bueler *et al.*, 1992). This mouse displayed a mixed background (B6129: C57BL6/J + 129Sv) and was further backcrossed with C57BL/6J mice to generate the B6.129 mouse line (Lledo *et al.*, 1996; Rangel *et al.*, 2009), and with FVB mice to generate the FVBN-$Prnp^{ZH1/ZH1}$ model (Lledo *et al.*, 1996) in order to reduce the 129/Sv-associated genes. However, the generated lines were systematically confounded by the *Prnp*-linked loci polymorphic region containing numerous 129/Sv-associated "*flanking genes*" (FG) close to *Prnp* deletion (de Almeida *et al.*, 2005; Nuvolone *et al.*, 2013). In fact, after crossing $Prnp^{ZH1/ZH1}$ mice with C57BL/6J for more than ten generations to reduce FG, a remnant of ≈ 2-5 % of the 129/Sv genome markers persisted in B6.129 mice (Carulla *et al.*, 2015; Nuvolone *et al.*, 2013; Sparkes *et al.*, 1986). More relevantly, FGs were also present in several mouse models derived from B6129 or B6.129 background, including

overexpressing mice (Fischer *et al.*, 1996), mice with cell-specific PrP^C expression (Flechsig *et al.*, 2003), and deletion mutants (Hara *et al.*, 2018; Shmerling *et al.*, 1998). The number of the FG mapping in chromosomes 2 and 4 was 62, related to different functions (i.e., cancer, depression, anxiety, among others (Nuvolone *et al.*, 2013). Thus, we consider that most of the physiological phenotypes attributed to the *Prnp* absence or overexpression in these mouse lines carrying FG need to be revaluated and confirmed in other FG-free models. As an example, in previous studies, we and others demonstrated that these FGs masked the real neuroprotective function of PrP^C against kainate administration *in vivo* (Rangel *et al.*, 2007; Rangel *et al.*, 2009; Striebel *et al.*, 2013; Walz *et al.*, 1999). Although a full description of the FG-associated effects in a null *Prnp* background is not available, one of these FGs is the signal regulatory protein alpha (Sirpα), an important regulator of several innate immune functions (Brown and Frazier, 2001). Although prion disease evolution is not modified in *Sirp*$\alpha^{0/0}$ mice (Nuvolone *et al.*, 2017a), it has been clearly demonstrated that Sirpα is mainly responsible for a phagocytic function previously attributed to PrP^C (de Almeida *et al.*, 2005; Nuvolone *et al.*, 2013). The number of functions misattributed to PrP^C increased when a recent study described a substrain-related dependence of Cu(I)-ATPase activity among *Prnp*$^{0/0}$ mice related to the 129/Sv FGs and not PrP^C (Adao-Novaes *et al.*, 2020).

In neurons, PrP^C is transported along axons (Encalada *et al.*, 2011) and enriched at the synaptic terminal, where it has been related to glutamate receptors (NMDA-R, AMPA, GluK2, and mGluR5) and anchoring proteins such as PSD-95 (i.e., (Carulla *et al.*, 2011; Ferreira *et al.*, 2017; Khosravani *et al.*, 2008)). However,

due to the different mouse strains used and some experimental differences, the involvement of PrP^C in neurotransmission is still elusive. For example, different studies reported reduced (Collinge *et al.*, 1994; Criado *et al.*, 2005; Curtis *et al.*, 2003; Manson *et al.*, 1995), normal (Lledo *et al.*, 1996), or enhanced (Maglio *et al.*, 2006; Rangel *et al.*, 2009) long-term potentiation (LTP) in *Prnp*$^{0/0}$ mice compared to wild-type mice. Following these descriptions, the consequences of *Prnp* absence in memory, learning, and behavior include variable results in studies using mice carrying FGs (i.e., (Bueler *et al.*, 1992; Coitinho *et al.*, 2003; Fainstein *et al.*, 2016; Lipp *et al.*, 1998; Schmitz *et al.*, 2014b)) or not (i.e., (Criado *et al.*, 2005; Manson *et al.*, 1994)).

In the present study, we focused our attention on reexamining some PrP^C functions associated with neurotransmission, learning, and behavior, taking advantage of a recently generated *Prnp*$^{0/0}$ mouse model: the Zürich 3 (*Prnp*$^{ZH3/ZH3}$) (Nuvolone *et al.*, 2016). This co-isogenic mouse was generated in a pure C57BL/6J background using TALEN technology (Nuvolone *et al.*, 2016) and it is resistant to prion infection (Nuvolone *et al.*, 2017b). Here we performed a set of behavioral tests to analyze *Prnp*$^{ZH3/ZH3}$ mouse activity, learning, and memory capabilities. In addition, basic synaptic functions, kainate-mediated excitability, and LTP induction were evaluated electrophysiologically in alert behaving mice. Finally, PrP^C roles during neuronal differentiation and activity were also evaluated in primary cortical cultures. Results indicate that adult *Prnp*$^{ZH3/ZH3}$ mice display reduced motility and anxiety-like behavior. They also fail to acquire different instrumental learning tasks. In addition, our experiments show that hippocampal CA3-CA1 *Prnp*$^{ZH3/ZH3}$ synapse cannot induce LTP, most likely due to an exacerbated endogenous excitability, further corroborated *in vivo* after kainate

injections. Finally, our *in vitro* experiments shows that the absence of PrP^C delayed the development of neuronal network maturation and reduced neuronal bursting using GCaMP6. Lastly, our results are sustained by the observed alteration in the expression patterns of several genes associated with neuronal system function and synaptic protein-protein interactions in the $Prnp^{ZH3/ZH3}$ hippocampus by an RNAseq analysis and its qPCR validation.

Material and methods

Animals

Adult C57BL/6J mice ($Prnp^{+/+}$) were purchased from Charles River Laboratories (Paris, France). $Prnp^{ZH3/ZH3}$ mice line was provided by A. Aguzzi (Switzerland) (see (Nuvolone *et al.*, 2016) for details). $Prnp^{ZH1/ZH1}$ mice (Bueler *et al.*, 1992) were purchased from the European Mouse Mutant Archive (EMMA, Monterotondo, Italy). A total of 156 adult (3-5 months old) male mice (ZH3: $Prnp^{+/+}$= 67 and $Prnp^{0/0}$= 69; ZH1: $Prnp^{+/+}$= 10 and $Prnp^{0/0}$ = 10) were used in the present study. In ZH1 mouse experiments, null $Prnp^{ZH1/ZH1}$ and control mice ($Prnp^{+/+}$) were obtained by crossing heterozygous $Prnp^{+/ZH1}$ miceto obtain a mixed background (B6.129). All experiments were performed following the protocols and guidelines of the Ethical Committee for Animal Experimentation (CEEA) of the University of Barcelona. CEEA of the University of Barcelona approved the protocol for using animals in this study (CEEA approval #276/16 and 141/15). Behavioral and electrophysiological studies were performed following the guidelines of the European Union Council (2010/276:33-79/EU) and current Spanish regulations (BOE 34:11370-421, 2013) for the use of laboratory animals in chronic experiments. Experiments were also approved by the Ethics

Committee for Animal Care and Handling of the Pablo de Olavide University (UPO-JA 06/03/2018/025).

Behavioral studies

A total of 118 animals were used in these sets of experiments (ZH3: *Prnp*$^{+/+}$= 49 and *Prnp*$^{ZH3/ZH3}$ = 49; ZH1: *Prnp*$^{+/+}$= 10 and *Prnp*$^{ZH1/ ZH1}$ = 10). Mice were housed alone in boxes on a 12/12 h light/dark cycle with constant ambient temperature (21±1 ºC). Water and food were provided *ad libitum* except for the instrumental learning tests (see below).

Nest building

For this test, a total of 14 mice (3 months old) were used (*Prnp*$^{ZH3/ZH3}$ = 7 and *Prnp*$^{+/+}$ = 7). On the first day of testing, one piece of tissue paper (36 x 12 cm) was placed in the cage to facilitate nest building (Supplementary Figure 1). The presence and the quality of each nest were photo-documented and evaluated the following day according to a modified five-point scale using the method described by Deacon (Deacon, 2006). Two different blinded researchers evaluated the nest generated by each mouse. Data are presented as the mean ± S.E.M. in (Supplementary Figure 1). The statistical analysis was performed with the Mann-Whitney non-parametric test (GraphPad Prism 8 software).

Open field test

In this test, *Prnp*$^{ZH1/ZH1}$ mice were not used since a detailed study was already developed using this model (Schmitz *et al.*, 2014b; Schmitz *et al.*, 2014c). In our experiments, mice (*Prnp*$^{+/+}$ = 49 and *Prnp*$^{ZH3/ZH3}$ = 49) were placed in a square open field altimeter box (35 × 35 × 25 cm, Cibertec, Madrid, Spain). The field had

a grid (16 x 16 cm) of infrared lasers on the XY axis and one on the Z-axis. Locomotor activity was measured for 15 min in mice with the MUX-XYZ16L software. Mice were placed in the box's periphery for 15 min for two consecutive days, and their behavior recorded. The first day was considered a training session to reduce mouse anxiety associated with manual handling, and the data analyzed and displayed in the manuscript corresponded to the second session. The system inferred mouse activity by counting laser intersections. For anxiety-related behavior measurement, the center (inner) square of the field (10 x 10 cm) was considered as the central zone and the rest of the square as the peripheral (outer) zone (Seibenhener and Wooten, 2015) (see Figure 1A). For quantification and to distinguish motility from exploratory behavior, it was considered that a mouse spent time in one of the regions (center *vs.* periphery) if it remained in the region at least 3 s. Rearing episodes were considered when the animal stood up for at least 3 s, and immobility episodes if immobile for an additional 3 s. Obtained data were analyzed, and the sum of the crossed X and the Y axes are presented together to show total mouse mobility in the experiments. Time spent in the maze periphery zones measures thigmotaxis or wall-hugging behavior and indicates anxiety-related behavior (Seibenhener and Wooten, 2015). Data are presented as the mean ± S.E.M. The statistical analysis was performed with a *T*-test or Mann-Whitney non-parametric test (GraphPad Prism 8 software). The asterisks indicate significant differences: $^{**}p < 0.01$ and $^{***}p < 0.001$. The arena and the walls were cleaned with soap and ethanol between trials to remove olfactory cues between experiments.

Operant conditioning tests

The instrumental learning tests were performed as described in previous studies of our group (Madronal *et al.*, 2010; Hasan *et al,* 2013). Six Skinner boxes were used simultaneously (12.5 x 13.5 x 18.5 cm; MED Associates, St. Albans, VT, USA). Each Skinner box was housed in a sound-attenuating cubicle (90 x 55 x 60 cm) constantly exposed to white noise (± 45 dB) and dim light (Cibertec, S.A, Madrid, Spain). The boxes had a trough to receive food pellets (Noyes formula P; 45 mg; Sandown Scientific, Hampton, UK) by pressing a lever. Before the test, mouse food availability was monitored for seven days to reduce initial mouse weight to 85%. First, mice (ZH3: $Prnp^{+/+}$ = 49 and $Prnp^{ZH3/ZH3}$ = 49; and ZH1: $Prnp^{+/+}$ = 10 and $Prnp^{ZH1/ZH1}$ = 10) were trained to press the lever to receive food pellets in a fixed-ratio (1:1) schedule. Seven daily sessions (20 min/each) were held. The boxes were cleaned with soap and ethanol (30%) between trials. Obtaining ≥ 20 pellets for two consecutive sessions was defined as the criterion to assume the learning criteria achievement. Following this first operant conditioning test, we increased the paradigm complexity to test the mice in a more demanding cognitive task for an additional 10 days. Only animals that met the learning criterion were tested (ZH3: $Prnp^{+/+}$ = 24 and $Prnp^{ZH3/ZH3}$ = 20; and ZH1 $Prnp^{+/+}$ = 8 and $Prnp^{ZH1/ZH1}$ = 5). The paradigm consisted of light (ON period) and dark periods (OFF period) randomly distributed during the session. The light was provided by a small light bulb located over the lever. During the ON period (20 s), lever presses were reinforced with food pellets at a ratio of 1:1. During the OFF period, lever presses were not rewarded and were penalized by adding ten additional seconds (20 s ± 10 s) to the next ON period. The number of lever presses during the different conditioning paradigms was monitored and recorded with the MED-PC program (MED Associates, St. Albans, VT, USA). Statistical

analysis was carried out using two-way ANOVA with repeated measures and Bonferroni's multiple comparisons test (GraphPad Prism 8 software). Asterisks indicate significant differences: $^{**}p < 0.01$; and $^{***}p < 0.001$. Data are presented as the mean ± S.E.M., or as a percentage (as indicated in each Figure).

Object recognition test

The object recognition test was performed in a homemade arena (30 x 25 x 20 cm), as described (Clarke *et al.*, 2010). A total of 23 *Prnp*$^{+/+}$ and 24 *Prnp*$^{ZH3/ZH3}$ mice were analyzed. Additionally, 6 *Prnp*$^{ZH1/ZH1}$ mice were also used with 7 *Prnp*$^{+/+}$ counterparts. The test consisted of four phases of 10 min/each. First, animals were habituated to the field without any object (habituation session). One hour later, two identical plastic objects were placed in the center of the arena for the training session. A short-term memory test was performed 2-3 h later by changing one of the objects (see Supplementary Figure S2). ZH1 mouse mobility was expressed as the number of rearing episodes during the habituation session. The arena and the objects were cleaned with soap and (30 %) ethanol between trials to remove olfactory cues. Mouse behavior was recorded with a video camera placed over the arena, and these recordings were used to measure the exploratory behavior blindly. Sniffing and gently touching the objects were counted as exploratory behavior. To further support increased anxiety levels in the *Prnp*$^{ZH3/ZH3}$ mice, fecal bodies left in the maze during the habituation session were counted by the observer once the test subject was removed since it has been demonstrated that highly emotional animals exhibit increased defecation (Seibenhener and Wooten, 2015). Statistical analysis was performed with the

Mann-Whitney non-parametric test (GraphPad Prism 8 software). Data are presented as the mean ± S.E.M. or as a percentage (indicated in each Figure).

Mouse surgery

A total of 98 adult male mice were implanted with stimulating and recording electrodes (*Prnp*$^{+/+}$ = 49 and *Prnp*$^{ZH3/ZH3}$ = 49). Four of them died during surgery, and 33 mice were excluded because of the inability to obtain reliable and clean recordings. Thus, the experiments were performed with 61 mice (*Prnp*$^{+/+}$ = 31 and *Prnp*$^{ZH3/ZH3}$ = 30). Surgery was performed as described in (Gruart et al., 2006; Medrano-Fernandez *et al.*, 2018; Rangel *et al.*, 2009). Mice were deeply anesthetized with ketamine (35 mg/kg) and xylazine (2 mg/kg), and electrodes were aimed at the right dorsal hippocampus. Two recording electrodes were implanted in the *stratum radiatum* of the CA1 area (2.2 mm caudal to Bregma, 1.2 mm lateral, and 1.3 mm ventral), and two stimulating electrodes were implanted in the Schaffer collateral pathway of the CA3 region (1.5 mm posterior to Bregma, 2 mm lateral, and 1.3 mm ventral). Electrodes were made of 50 µm Teflon-coated tungsten wires (Advent Research, Eynsham, UK). Electrode localizations were checked according to the field excitatory postsynaptic potential (fEPSP) profile evoked by a single stimulation. A silver wire was fixed to the skull as ground. All the wires were soldered to a six-pin socket (RS Amidata, Madrid, Spain) fixed to the skull with dental cement. Recordings were started at a minimum of one week after the surgery.

Electrophysiology recordings

Six animals were recorded at the same time. Each animal was placed in a small plastic cubicle (5 x 5 x 10 cm) inside a large Faraday box (30 x 30 x 20 cm). fEPSPs were recorded with a high impedance probe (2 x 10^{12} Ω, 10 pF) using differential amplification at a bandwidth of 0.1 Hz-10 kHz (P511, Grass-Telefactor, West Warwick, RI, USA). For each experiment, artefactual recordings were discarded. The stimulation intensity threshold of each animal was set with paired-pulse stimulations at 40 ms of inter-stimulus interval. The stimulus intensity was set to 40-60% of the amount necessary to evoke a suturing response. These intensity values were used for all the experiments.

Paired-pulse stimulation

For synaptic facilitation experiments, 51 mice ($Prnp^{+/+}$ = 27 and $Prnp^{ZH3/ZH3}$ = 24) were stimulated at Schaffer collaterals with a pair of pulses at different inter-stimulus intervals (10, 20, 40, 100, 200, and 500 ms) at threshold intensities previously defined for each mouse. For all the inter-pulse intervals, the stimulations were repeated ten times. Data are represented as the mean percentage increases of fEPSP2 from fEPSP1 recordings (fEPSP2 / fEPSP1 x 100) ± S.E.M.

Input/output curves

Schaffer collaterals of 29 mice ($Prnp^{+/+}$ = 14 and $Prnp^{ZH3/ZH3}$ = 15) were stimulated with paired pulses at 20 increasing intensities (0.02 to 0.04 mA increased in steps of 0.02 mA) at 40 ms of inter-stimulus interval. For all the selected intensities, the stimulations were repeated ten times. Data are represented as the mean of fEPSP slopes (V /s) ± S.E.M. The same data are presented as the mean of

paired-pulsed ratio (PP ratio) ± S.E.M. PP ratio is the percentage of the increase of the fEPSP2 from fEPSP1 recordings (fEPSP2 / fEPSP1 x 100). The area under the curve (AUC) was calculated from the PP ratio of all the animals using GraphPad Prism 8 software. Statistical analysis was performed using the Mann-Whitney-Wilcoxon non-parametric test or two-way ANOVA with Bonferroni's multiple comparisons test (GraphPad Prism 8 software). The asterisks indicate significant differences: $^{*}p < 0.05$; $^{**}p < 0.01$; and $^{***}p < 0.001$ in the Figure.

Long-term potentiation experiments

In a first experimental step, fEPSP baseline values were evoked and recorded for 15 min, with paired-pulse stimulus presented every 20 s (40 ms inter-stimulus). Next, LTP was evoked with a high-frequency stimulation (HFS) protocol. HFS consisted of five trains of pulses at a rate of 1/s (200 Hz, 100 ms) with the same intensity as the baseline recording. The HFS was repeated six times at intervals of 1 min. After the HFS protocol, fEPSPs were recorded, as for baseline, for 1 h. The following four days, the recordings were repeated for 30 min. fEPSPs and 1 V rectangular pulses corresponding to stimulus presentations were saved on a PC using an analog/digital converter (CED 1401 Plus, Cambridge, England). Data were analyzed offline using Spike2 and Signal 5.04 software with home-made representation programs (Gruart et al., 2006; Madroñal *et al.*, 2009). Data are presented as the mean of the percentage compared to the baseline ± S.E.M. The statistical analysis was performed using two-way ANOVA with Bonferroni's multiple comparisons test (GraphPad Prism 8 software). The asterisks and symbols indicate significant differences: $^{*}p < 0.05$; $^{**}p < 0.01$; and $^{***}p < 0.001$; $^{\#\#}p < 0.01$; and $^{\#\#\#}p < 0.001$.

Kainate-induced epilepsy and seizure analysis

Adult (3-4 months old) male mice were used for these sets of experiments ($Prnp^{+/+}$ = 18 and $Prnp^{ZH3/ZH3}$ = 20) essentially as described in (Carulla *et al.*, 2015). A kainate (KA) (Sigma, Darmstadt, Germany) solution was freshly prepared for each experiment in 0.1 M phosphate buffer. Mice were injected with KA (10 mg/kg b.w.) three times: at 0 min, 30 min, and 60 min. After the first injection, mice were placed in clean boxes (1-3 mice/box). The presence of epileptic seizures was monitored *in situ* and recorded with a video camera for 3 h after drug administration. Seizure severity was scored in grades following the following criteria: grade I-II: hypoactivity and immobility; grade III-IV: hyperactivity and scratching; grade V: loss of balance control and intermittent convulsions; grade VI: continuous seizures and bouncing activity (also reported as blinking episodes or ”*pop-corn*“ behavior). Data are presented as the mean ± S.E.M. or as a percentage (as indicated in each Figure). Statistical analysis was performed with the Mann-Whitney non-parametric test (GraphPad Prism 8 software). The asterisk indicates significant differences: $*p < 0.05$ in the Figure.

RNAseq and RT-qPCR

Libraries were prepared using the TruSeq Stranded mRNA Sample Prep Kit v2 (ref. RS-122-2101/2) according to the manufacturer's protocol. Briefly, 500 ng of total RNA was used for poly(A)-mRNA selection using Oligo (dT) magnetic beads and subsequently fragmented to approximately 300bp. cDNA was synthesized using reverse transcriptase (SuperScript II, Invitrogen) and random primers. The second strand of the cDNA incorporated dUTP in place of dTTP. Double-stranded DNA was further used for library preparation. dsDNA was subjected to A-tailing

and ligation of the barcoded Truseq adapters. All purification steps were performed using AMPure XP Beads. Library amplification was performed with PCR using the primer cocktail supplied in the kit. Final libraries were analyzed using Agilent DNA 1000 chip to estimate the quantity, check the size distribution, and then quantify by qPCR using the KAPA Library Quantification Kit (KapaBiosystems) before amplification Illumina's cBot. Libraries were sequenced 1 x 50bp on Illumina's HiSeq 2500.

The quality of the fast files was checked using the FastQC software (http://www.bioinformatics.babraham.ac.uk/projects/fastqc/). An estimation of ribosomal RNA in the raw data was obtained with riboPicker (Schmieder *et al.*, 2012). Reads were aligned with the STAR mapper (Dobin *et al.*, 2013) to release M14 of the Mus musculus Gencode version of the genome (GRMm38/mm10 assembly) (https://www.gencodegenes.org/mouse/release_M14.html). A raw count of reads per gene was also obtained with STAR (-quantMode TranscriptomeSAM GeneCounts option). The R/Bioconductor package DESeq2 (Huber *et al.*, 2015; Love *et al.*, 2014) was used to assess differential expression between experimental groups (Wald statistical test + false discovery rate correction). Prior to processing the differential expression analysis, genes for which the sum of raw counts across all samples was less than two were discarded. Deregulated genes with a padj <0.05 were used to disclose relevant pathway alterations in the REACTOME pathway database gene expression. For RT-qPCR validations, cDNA was obtained with a High-Capacity cDNA Reverse Transcription kit (Applied Biosystems) following the supplier's instructions. RT-qPCR reactions contained 4.5 µL cDNA, mixed with 0.5 µL 20X TaqMan Gene

Expression Assays and 5 µL of 2X TaqMan Universal PCR Master Mix (Applied Biosystems) for a final volume of 10 µL. TaqMan probes used were: *Grin2b* Mm00433820_m1, *Gabrr2* Mm00433507_m1, *Kacnj6* Mm01215650_m1, *Kcna1* Mm00439977_s1, *Kcnj2* Mm00434616_m1, *Kcnq3* Mm00548884_m1 (Applied Biosystems). *Actb* Mm02619580_g1 and *Aars* Mm00507627_m1 were used as endogenous controls. The assay was performed using technical duplicates per sample in 384-well optical plates with ABI Prism 7900 Sequence Detection system (Applied Biosystems, Life Technologies) following the supplier's parameters: 50°C for 2 min, 95°C for 10 min, and 40 cycles of 95°C for 15 s and 60°C for 1 min. The Sequence Detection Software (SDS version 2.2.2, Applied Biosystems) was used for data processing. It was further analyzed with the ΔΔCt method, which consists in obtaining ΔCt by normalizing each target gene to its endogenous control, followed by subtracting the mean-ΔCt of the control group samples to each ΔCt to obtain ΔΔCt values, and finally using these ΔΔCt values as the negative exponent with base 2, thereby obtaining fold change per sample.

Fluoro-Jade B staining

Mice were perfused seven days after the kainate administration with 4% paraformaldehyde (PFA) dissolved in 0.1 M phosphate buffer (pH = 7.3-7.4). Brains were dissected and postfixed overnight with the same fixative solution. The following day, they were cryoprotected in 0.1 M phosphate buffer containing 30% sucrose (w/v). After freezing in dry ice, 50 µm thick coronal sections were obtained with a freezing microtome (Leica, Wetzlar, Germany). Sections containing the dorsal hippocampus were selected and rinsed in 0.1M phosphate buffer and mounted on gelatin-coated slides. The slides containing sections were

dried at 37ºC overnight. The following day, they were heated at 50ºC for 45 min before staining to improve adhesion. The staining started with pretreatment for 3 min in absolute alcohol, followed by 1 min in 70% ethanol and 1 min in deionized water. After that, they were oxidized in a solution of 0.06% $KMnO_4$ for 15 min. Following three rinses (2 min/each) in deionized water, they were incubated in a solution of 0.001% Fluoro-Jade B (Chemicon, Temecula, CA, USA) containing 0.05% of DAPI in 0.1% acetic acid for 30 min. Finally, sections were rinsed in deionized water (3 min), dehydrated with ethanol, cleared with xylene, and coverslipped with Eukitt™ (Merck, Darmstadt, Germany). Sections were examined using an Olympus BX61 epifluorescence microscope equipped with a cooled DP12L camera (Hamburg, Germany).

Primary cortical cultures of *Prnp*$^{ZH3/ ZH3}$ and wild-type mice

Primary cortical cultures were fashioned from E16.5-E17.5 *Prnp*$^{+/+}$ and *Prnp*$^{ZH3/ZH3}$ mouse embryos, as explained elsewhere (Urrea *et al.*, 2018). Brains were removed from the skull and rinsed in cold Hank's balanced salt solution (HBSS) containing glucose (6.5 mg/ml). The meninges were removed, and the cortical lobes were isolated. Tissue pieces were treated with trypsin for 15 min at 37ºC. After the addition of horse serum followed by centrifugation, cells were isolated mechanically with a polished glass pipette after treatment with 0.025% DNAse for 10 min at 37ºC. One million cells were plated on a 35 mm ∅ glass-bottom gridded culture dish (Ibidi, Martinsried, Germany) previously coated with poly-D-lysine (Sigma-Aldrich, Darmstadt, Germany). Neurobasal™ medium supplemented with 6.5 mg/ml glucose, 2 mM glutamine, penicillin/streptomycin, 5% of horse serum, and B27 was used as a culture medium (all from Invitrogen-

Thermo Fisher Scientific, MA, USA). As *Prnp*$^{0/0}$-derived cells are sensitive to serum removal (Nishimura *et al.*, 2007), after 24 h, the serum was reduced to 2.5%. The medium was changed every two days. Horse serum was entirely removed on the eighth day of culture.

Calcium imaging in neuronal culture

Primary cortical neurons were infected 24 h after seeding with AAV9-Syntaxin-GCaMP6 (Chen *et al.*, 2013) (Watertown, MA, USA). In our cultures, the genetically encoded calcium indicators started to express 3-4 days after infection. Calcium changes in GCaMP6-expressing neurons were recorded at 8, 11, 13, and 15 days *in vitro* (DIV) using an Olympus IX71 inverted microscope (Hamburg, Germany), equipped with an ORCA-Flash 4.0 camera (Hamamatsu Photonics, Japan). During recording, the cells were maintained in a microscope stage incubator at 5% CO_2 and 37ºC (Okolab S.R.L., Italy). The same region of the culture was recorded throughout the days following the culture dish grid references. Images (1024 x 1024 pixels) were captured using a 20x objective and 470 nm wavelength (CoolLED's pE-300^{white}, Delta Optics, Madrid, Spain) every 100 ms for 8-10 min using the CellSens^{TM} software (Olympus) or the Micro-Manager Open Source Microscopy Software (https://micro-manager.org). Exposure levels and frequency were maintained between cultures and evaluation days. GCaMPC6 activity was measured in four different identified squares of each culture dish during these four days.

Neuronal activity traces, spike events, and network bursts

The recordings were analyzed offline using two MATLAB toolboxes: NETCAL (www.itsnetcal.com) (Orlandi *et al.*, 2014; Teller *et al.*, 2015) and NeuroCa (Jang and Nam, 2015). In NeuroCa, an automatic analysis was performed afterward to corroborate obtained NETCAL results. Using NETCAL, a highly contrasted image of the recording's average fluorescence was created, and regions of interest (ROIs) were automatically detected as those objects with a circular shape whose brightness was over a preset threshold. NETCAL and NeuroCa software rendered a similar number of ROIs and calcium traces. About 400 ROIs, uniformly covering the field of view, were typically identified per recording. The average fluorescence $Fi\,(t)$ in each ROI i along the recording was then extracted, corrected from global drifts and artifacts, and finally normalized as $(Fi\,(t) - F_{(0,i)}) / F_{(0,i)} = fi\,(t)$, where $F_{0,i}$ is the background fluorescence of the ROI. The time series of $fi\,(t)$ was analyzed with NETCAL to infer neuronal activation timing using the Schmitt trigger method. Our analysis used +2 S.E.M. of the baseline noise as the high threshold, +1.5 S.E.M. as the low threshold, and 200 ms as the minimum event length. Calcium traces were calculated, and raster plots of network activity were then constructed by representing the trains of detected neuronal spikes over time. Next, network bursts were analyzed to quantify the ability of the neuronal networks to exhibit collective dynamics, i.e., the collective activation of a group of neurons in a short time window. Bursts were investigated using two approaches. In the first approach, raster plots of spike events were scanned to detect collective occurrences in which at least 5% of the neurons in the network fired synchronously within a 500 ms window. This threshold of 5% was set to disregard random activations that coincided in time. In the second approach, the fluorescence time series of all neurons in the network were averaged. The

resulting trace was analyzed with the Schmitt trigger method to detect sufficiently strong fluorescence peaks associated with bursting episodes. Both approaches produced consistent results. Although the detected bursts contained a different number of participating neurons, this information was disregarded in the present analysis and treated later. The total number of detected network bursts divided by the recording duration reflected the culture's activity and was indicated as bursts/min.

The fraction of active neurons in the network was calculated as follows. All detected ROIs were assigned as neurons. After inferring the spike trains, those neurons exhibiting at least two spikes along the recording were considered active, and their number N_A set as a proxy of the healthy population in the neuronal network. The average fraction of active neurons in each condition was then determined as $f = N_A/N_T$, where N_T is the total number of detected ROIs.
At least ten videos of each genotype/day from different culture plates were consecutively analyzed. Data are presented as the mean of network burst/min ± S.E.M. Statistical analysis was performed using two-way ANOVA and Bonferroni's multiple comparisons test (GraphPad Prism 8 software). Asterisks indicate significant differences between *Prnp*$^{+/+}$ and *Prnp*$^{ZH3/ZH3}$ cultures at a given DIV: $^{*}p < 0.05$ and $^{***}p < 0.001$. The # symbols indicate significant differences between a given DIV with the initial value at 8 DIV: $^{\#\#\#}p < 0.001$.

Results

The absence of PrP^C has been related to deficiencies in behavior, learning, and memory in several mouse models with different results (Bueler *et al.*, 1992; Criado *et al.*, 2005; Gadotti *et al.*, 2012; Salazar *et al.*, 2017). In order to evaluate the implication of PrP^C in systemic behavioral tasks, we took advantage of the new knock-out model, the $Prnp^{ZH3/ZH3}$ mouse. First, we analyzed the nest building capacity between $Prnp^{ZH3/ZH3}$ *vs.* wild-type mice as an indicator of mouse welfare. In contrast to Schmitz *et al.,* using $Prnp^{ZH1/ZH1}$ mice (reviewed in (Schmitz *et al.*, 2014c)), results showed a slightly increased but not significantly so nest-building capacity in $Prnp^{ZH3/ZH3}$ compared to controls ($Prnp^{ZH3/ZH3}$ = 3.81 ± 0.64 *vs.* *Prnp*+/+ = 3.00 ± 0.41) (Supplementary Figure 1), suggesting that the two genotypes showed similar welfare conditions (Jirkof, 2014).

Reduced activity, increased thigmotaxis, and anxiety-related behavior in $Prnp^{ZH3/ZH3}$ mice

First, we performed the open field test to measure mouse activity and interaction with the environment. $Prnp^{+/+}$ and $Prnp^{ZH3/ZH3}$ mice were individually placed in the open field arena for 15 min, and their activity was evaluated on the X-Y-Z axes (Figure 1A). $Prnp^{ZH3/ZH3}$ mice showed significantly reduced displacement in the field ($Prnp^{+/+}$ = 3725 ± 93 a.u. *vs.* $Prnp^{ZH3/ZH3}$ = 3370 ± 95 a.u.; $^{**}p = 0.009$; *T-test*) (Figure 1B). Anxiety and stress increased the thigmotaxis behavior and the natural aversion to exploring the inner square of the field during the test (Seibenhener and Wooten, 2015). So, to evaluate anxiety-like behavior in the $Prnp^{ZH3/ZH3}$ mice, we measured this thigmotaxis performance as the time spent in

the center (inner region) *vs.* the periphery (outer region) for each mouse (Figure 1A). *Prnp*$^{+/+}$ mice spent the same amount of time in the two regions, while *Prnp*$^{ZH3/ZH3}$ animals remained significantly more time in the periphery close to the walls, suggesting an apprehension of the center of the field that reflects an anxiety-like behavior (*Prnp*$^{+/+}$: Center = 303.3 ± 14.5 *vs.* Periphery = 345.7 ± 18,0; and *Prnp*$^{ZH3/ZH3}$: Center = 288.2 ± 15.1 *vs.* Periphery = 394.3 ± 20.3; mean ± S.E.M., *p = 0.071 and ****p < 0.0001 respectively; *T-test*) (Figure 1C). Stressed behavior was also assessed by counting the number of rearing and immobility episodes. *Prnp*$^{ZH3/ZH3}$ mice displayed significantly fewer rearing episodes (*Prnp*$^{+/+}$ = 52 ± 2 *vs.* *Prnp*$^{ZH3/ZH3}$ = 26.6 ± 1.7; mean ± S.E.M., ****p < 0,0001; *T-test*) and more immobility episodes (*Prnp*$^{+/+}$ = 6.6 ± 1.2 *vs.* *Prnp*$^{ZH3/ZH3}$ = 12.4 ± 0.9; mean ± S.E.M., ****p < 0.0001; Mann-Whitney test) confirming an anxiety-like behavior (Figure 1D).

Prnp$^{ZH3/ZH3}$ mice and _Prnp_$^{ZH1/ZH1}$ failed to acquire instrumental learning tasks

Our next goal was to examine the capabilities of *Prnp*$^{ZH3/ZH3}$ mice in performing highly demanding learning tasks. Instrumental learning capabilities were tested with operant conditioning in the Skinner box (Figure 2). Collected data were compared to those obtained using *Prnp*$^{ZH1/ZH1}$ mice (Supplementary Figure 2). Thirty-one percent of *Prnp*$^{ZH3/ZH3}$ mice did not reach the learning criterion (to obtain ≥ 20 pellets for two consecutive sessions) at the end of the training session. In contrast, all *Prnp*$^{+/+}$ mice (100%) met the selected criterion from the 6th session (Figure 2A). Similarly, in a second set of experiments using *Prnp*$^{ZH1/ZH1}$ mice (*Prnp*$^{+/+}$ = 10 and *Prnp*$^{ZH1/ZH1}$ = 10), 50% of *Prnp*$^{ZH1/ZH1}$ mice failed to reach the criterion, but 80% of wild-type mice reached it at the end of the

sessions (Supplementary Figure 2). These results strongly suggest that mice lacking *Prnp* (ZH1 and ZH3 backgrounds) present evident instrumental learning deficiencies. Also, $Prnp^{+/+}$ mice pressed the lever significantly more times from session 3 onwards than the $Prnp^{ZH3/ZH3}$ animals (Session 3: $Prnp^{+/+}$ = 40.2 ± 5.1 *vs.* $Prnp^{ZH3/ZH3}$ = 23.3 ± 3.2, ***p = 0.0023; Session 4: $Prnp^{+/+}$ = 53.0 ± 3.9 *vs.* $Prnp^{ZH3/ZH3}$ = 29.4 ± 3.1, ****p < 0.0001; Session 5: $Prnp^{+/+}$ = 55.1 ± 3.3 *vs.* $Prnp^{ZH3/ZH3}$ = 36.1 ± 3.9, ***p = 0.0003; Session 6: $Prnp^{+/+}$ = 70.5 ± 4.1 *vs.* $Prnp^{ZH3/ZH3}$ = 38.3 ± 3.9 ****p < 0.0001; Session 7: $Prnp^{+/+}$ = 59.9 ± 2.3 *vs* $Prnp^{ZH3/ZH3}$ = 39.6 ± 3.5, ****p < 0.0001; two-way ANOVA with Bonferroni's multiple comparisons test) (Figure 2B). However, as we saw in the open field test, they displayed considerable inactive behaviors (Figure 1). To distinguish the reduction of activity from real learning deficits, 44 mice ($Prnp^{+/+}$ = 24 and $Prnp^{ZH3/ZH3}$ = 20) were subjected to a more complex operant conditioning paradigm, the light ON/light OFF task (see Material and methods). As expected, the total number of lever pulses during the OFF period was higher in the $Prnp^{+/+}$ mice and drastically reduced along with sessions (Session 1 = 134.8 ± 13.3 *vs.* Session 10 = 39.7 ± 5.2) (Figure 2C). In parallel, $Prnp^{+/+}$ mice increased the number of pulses in the ON period (Session 1 = 26.9 ± 1.8 *vs.* Session 10 = 45.7 ± 2.8) (Figure 2C). In contrast, $Prnp^{ZH3/ZH3}$ mice showed a reduced decrease of pulses in the OFF period (Session 1 = 73.2 ± 11.7 *vs.* Session 10 = 26.5 ± 3.9) and an incipient increase in the ON period (Session 1 = 23.4 ± 1.6 *vs.* Session 10 = 31.1 ± 2.9) (Figure 2D). Learning capacity, measured as the difference in the curve slope during ON or OFF periods, was drastically reduced in $Prnp^{ZH3/ZH3}$ mice (OFF: $Prnp^{+/+}$ = -12.5, R^2 = 0.90; $Prnp^{ZH3/ZH3}$ = -5.9, R^2 = 0.92 ; ON: $Prnp^{+/+}$ = 2.3, R^2 = 0.96; $Prnp^{ZH3/ZH3}$ = 0.8, R^2 = 0.48) (Figures 2C-D). These differences

show that *Prnp*$^{ZH3/ZH3}$ mice failed to learn to avoid OFF periods and push the lever during the ON periods, indicating that PrP^{C} seems to be necessary to properly acquire instrumental learning tasks. A similar study was developed using *Prnp*$^{ZH1/ZH1}$ mice, and the task accuracy ratio ((lever presses during light ON – lever presses during light OFF)/(total number of lever presses)) was evaluated. At the end of the experiment (sessions 7 and 8), the *Prnp*$^{ZH1/ZH1}$ mice showed lower values than wild-type mice (session 7: *Prnp*$^{+/+}$ = 0,31 *vs. Prnp*$^{ZH1/ZH1}$ = -0.02; session 8: *Prnp*$^{+/+}$ = 0,54 *vs. Prnp*$^{ZH1/ZH1}$ = 0.1), reinforcing the notion that the absence of PrP^{C} decreases the instrumental learning goals in mutant mice (Supplementary Figure 2).

Finally, episodic memory was evaluated with the object recognition test. In our experiments, several *Prnp*$^{ZH3/ZH3}$ mice interacted with the objects for just a few seconds (Supplementary Figure 3). Therefore, we ruled out this approach because *Prnp*$^{ZH3/ZH3}$ mouse inactivity, probably related to the anxiety-like behavior we observed in the open field test, implies reducing interactions with the objects that rendered the learning results unreliable. To further support increased anxiety levels in the object recognition test, the fecal bodies left in the arena after the habituation session were counted by the observer once the test subject was removed. *Prnp*$^{ZH3/ZH3}$ mice exhibited significant increases in fecal bodies present when compared to wild-type mice (*Prnp*$^{ZH3/ZH3}$ = 4.76 ± 0.56 *vs. Prnp*$^{+/+}$ = 1.29 ± 0.52. mean ± S.E.M., **** $p < 0.0001$, *T-test*) (Supplementary Figure 3). Results correlate with the thigmotaxis levels measured in the *Prnp*$^{ZH3/ZH3}$ mice and indicate that the knock-out mice showed increased emotionality and anxiety compared to their wild-type counterparts. This was in contrast to what was observed using *Prnp*$^{ZH1/ZH1}$mice. In the habituation session, knock-out mice

showed a significant decrease in rearing episodes (*Prnp*$^{+/+}$ = 43.21 ± 10.01 *vs*. *Prnp*$^{ZH1/ZH1}$ = 15.7 ± 2.8, mean ± S.E.M., ****$p < 0.0001$, *T-test*). No changes were observed in the training phase, but *Prnp*$^{ZH1/ZH1}$ showed a tendency to decreased time (although non-significant, $p = 0.053$) analyzing the second object ((second - first) / total) compared to wild-type mice (*Prnp*$^{+/+}$ = 0.3 ± 0.15 *vs. Prnp*$^{ZH1/ZH1}$ = -0.17 ± 0.15, mean ± S.E.M.) (Supplementary Figure 3).

Increased excitability in *Prnp*$^{ZH3/ ZH3}$ Schaffer collateral pathway

PrP^{C} has been described as a regulator of glutamatergic neurotransmission in the hippocampus (e.g., (Khosravani *et al.*, 2008; Rangel *et al.*, 2009)). Therefore, we analyzed the activation of the well-characterized hippocampal Schaffer collateral pathway (CA3-CA1 synapses). Stimulating and recording electrodes were permanently implanted in the CA3 and CA1 regions, allowing us to record and quantify the evoked fEPSPs in living behaving mice (Figure 3A). First, we evaluated the synaptic facilitation in CA1 triggered by paired stimulation pulses in the CA3 area (Figure 3B). Paired-pulse facilitation was tested in *Prnp*$^{+/+}$ (n = 27) and *Prnp*$^{ZH3/ZH3}$ (n = 24) mice at different inter-stimulus intervals (from 10 to 500 ms). This approach generates a higher fEPSP from the second stimulus (fEPSP2) than from the first (fEPSP1) at short intervals due to presynaptic facilitation. In our experiments, no differences were observed between *Prnp*$^{+/+}$ and *Prnp*$^{ZH3/ZH3}$ facilitation (Figure 3B), suggesting that PrP^{C} does not participate in presynaptic mechanisms related to synaptic facilitation (see Madroñal et al., 2009).

Next we analyzed the consequences of PrP^{C} deficiency in hippocampal synaptic excitability (Figure 3C-D). The slope of fEPSP facilitation evoked by paired-pulse

(40 ms inter-stimulus interval) stimulation was measured at increasing intensities (from 0.02 to 0.4 mA). In *Prnp*$^{+/+}$ (n = 14) mice, fEPSP1 and fEPSP2 increased steadily more or less in parallel after 0.18 mA stimulation, reaching asymptotic values at 0.32 mA (Figure 3C). fESPS2 was significantly greater in three stimulation intensities before arriving at the asymptotic values showing synaptic facilitation (0.24 mA: fESPS1 = 0.57 ± 0.1 V/s and fEPSP2 = 1.19 ± 0.2 V/s, ***p* = 0.030; 0.26 mA: fESPS1 = 0.70 ± 0.1 V/s and fEPSP2 = 1.32 ± 0.2 V/s, ***p* = 0.031; 0.24 mA: fESPS1 = 0.80 ± 0.1 V/s and fEPSP2 = 1.42, ± 0.2 V/s, ***p* = 0.028, mean ± S.E.M., two-way ANOVA + Bonferroni's multiple comparisons test). From 0.26 mA stimulation, fEPSP1 and fEPSP2 were statistically equal in *Prnp*$^{+/+}$ mice; thus there was no synaptic facilitation at high intensities (Figure 3C). This phenomenon has been described as a putative protective mechanism in high intensity insults to maintain hippocampal homeostasis (Madroñal *et al.*, 2009). In contrast, in *Prnp*$^{ZH3/ZH3}$ (n = 15) mice, fEPSP1 and fEPSP2 did not increase in parallel, showing exacerbated facilitation and suggesting the absence of this protective mechanism (Figure 3D). fEPSP2 was significantly greater than fEPSP1 at higher intensities (i.e.: 0.28 mA: fESPS1 = 0.4 ± 0.1 V/s and fEPSP2 = 1.09 ± 0.2 V/s, ***p* = 0.010; 0.32 mA: fESPS1 = 0.57 ± 0.1 V/s and fEPSP2 = 1.5 ± 0.3 V/s, ****p* = 0.0002; 0.36 mA: fESPS1 = 0.67 ± 0.1 V/s and fEPSP2 = 1.73 ± 0.3 V/s, ****p* < 0.0001; 0.40 mA: fESPS1 = 0.9 ± 0.2 V/s and fEPSP2 = 1.73 ± 0.4 V/s, ****p* = 0.004; mean ± S.E.M., two-way ANOVA + Bonferroni's multiple comparisons test). *Prnp*$^{+/+}$ fEPSP1 increased steadily to greater asymptotic values than *Prnp*$^{ZH3/ZH3}$ fEPSP1 (from 0.3 mA stimulation ≈ 50% increased), but fEPSP2 were almost equal (fEPSP1: *Prnp*$^{+/+}$ ≈ 1.0 V/s; *Prnp*$^{ZH3/ZH3}$ ≈ 0.7 V/s and fEPSP2: *Prnp*$^{+/+}$ ≈ 1.5 V/s; *Prnp*$^{ZH3/ZH3}$ ≈ 1.6 V/s). Consequently, the

increase in fEPSP1 related to fEPSP2 was ≈50% in *Prnp*$^{+/+}$ individuals, but > 140% in their *Prnp*$^{ZH3/ZH3}$ counterparts.

Exacerbation of synaptic facilitation was clearly observed with the paired-pulsed (PP) ratio (fEPSP2/fEPSP1 x 100). At high intensities, the PP ratio was larger in the *Prnp*$^{ZH3/ZH3}$ connection (Figure 3E). The area under the curve (AUC) from 0.24 mA intensity was significantly lower in the *Prnp*$^{+/+}$ (*Prnp*$^{+/+}$ = 26.07 ± 4.0 a.u *vs.* *Prnp*$^{ZH3/ZH3}$ = 40.75 ± 7.1 a.u., mean ± S.E.M., **p* = 0.04; Mann-Whitney non-parametric test) (Figure 3F). These results indicate that PrP^{C} regulates neuronal excitability and synaptic homeostasis at high-intensity stimulations, suggesting a neuroprotective role.

High-frequency stimulation evoked epileptic seizures in *Prnp*$^{ZH3/ZH3}$ Schaffer collaterals but failed to increase LTP

As indicated, several studies reported differing data on LTP in *Prnp*$^{0/0}$ mice (see Introduction). So, to analyze LTP in *Prnp*$^{ZH3/ZH3}$ mice, we performed an LTP induction protocol based on high-frequency stimulation (HFS) (Figure 4). First, the baseline fEPSPs were recorded for 15 min, evoked by double pulses at an inter-stimulus interval of 40 ms. Afterward, the HFS protocol was presented. This consisted of five trains (200 Hz, 100 ms) of pulses (1/s) presented six times (1/min). Recordings were maintained for 60 min immediately after the HFS and repeated 30 min daily for four days from the HFS presentation session. *Prnp*$^{+/+}$ displayed significant LTP for both pulses (Figure 4A). fESPS1 and fESPS2 recordings were significantly larger than the baseline after the HFS, and this potentiation lasted for the five days of recording sessions. As expected, HFS reduced paired-pulsed facilitation the first day (see Madroñal et al., 2009).

However, from the second day, facilitation recovered steadily but with a range of increase from 350% to 150% with respect to fEPSP1 (i.e.: Baseline: fEPSP1 = 100%; fEPSP2 = 268.2 ± 43.1 %; Day 1: fEPSP1 = 478.3 ± 78.4 %; fEPSP2 = 441.1 ± 140.2 %; Day 3: fEPSP1 = 310.4 ± 47.0 %; fEPSP2 = 466.3 ± 106.7 %; mean ± S.E.M.) (Figure 4A). In contrast, *Prnp*$^{ZH3/ZH3}$ LTP induction was virtually absent and paired-pulsed facilitation was maintained (≈ 60%) from the first day (i.e.: Baseline: fEPSP1 = 100 %; fEPSP2 = 158.4 ± 23.0 %; Day 1: fEPSP1 = 153.43 ± 15.7 %; fEPSP2 = 224.3 ± 39.8 %; Day 3: fEPSP1 = 114.2 ± 11.9 %; fEPSP2 = 160.4 ± 23.8 %; mean ± S.E.M.) (Figure 4B).

In addition, *Prnp*$^{+/+}$ presented significantly larger fEPSP1 than *Prnp*$^{ZH3/ZH3}$ mice (i.e.: Day 1: *Prnp*$^{+/+}$ = 478.3 ± 78.3 % *vs.* *Prnp*$^{ZH3/ZH3}$ = 153.4 ± 15.7 %, ****p < 0,0001; Day 3: *Prnp*$^{+/+}$ = 399.9 ± 65.0 % *vs.* *Prnp*$^{ZH3/ZH3}$ = 131.8 ± 12.3 %, ****p = 0.0009; Day 5: *Prnp*$^{+/+}$ = 226.3 ± 29.4 % *vs.* *Prnp*$^{ZH3/ZH3}$ = 84.7 ± 8.0 %, *p = 0.034; two-way ANOVA, Bonferroni's multiple comparisons test) (Figure 4C). Following the same tendency, in *Prnp*$^{ZH3/ZH3}$ mice fEPSP2 was also smaller than in *Prnp*$^{+/+}$ (i.e.: Day 1: *Prnp*$^{+/+}$ = 441.1 ± 140.2 % *vs.* *Prnp*$^{ZH3/ZH3}$ = 224.3 ± 39.8 % ***p = 0.008; Day 3: *Prnp*$^{+/+}$ = 466.3 ± 106.7 % *vs.* *Prnp*$^{ZH3/ZH3}$ = 181.4 ± 25.9 % p = 0,05; Day 5: *Prnp*$^{+/+}$ = 433.1 ± 87.7 % *vs.* *Prnp*$^{ZH3/ZH3}$ = 133.53 ± 18.0 %; p = 0.06; two-way ANOVA + Bonferroni's multiple comparisons test) (Figure 4D). These results indicate that LTP increased fEPSPs in *Prnp*$^{+/+}$ connection but not in *Prnp*$^{ZH3/ZH3}$. These results were surprising and were not in accordance with previous publications in which *Prnp*$^{ZH1/ZH1}$ mice had even exacerbated LTP (Rangel *et al.*, 2009). In an attempt to explain these results, we checked the *in situ* registers in detail during the HFS protocol (Figure 4E). We observed that 55% of the *Prnp*$^{ZH3/ZH3}$ mice suffered from epileptic seizures due to HFS in contrast to

20% of the *Prnp*$^{+/+}$ mice (Figure 4F). The *Prnp*$^{ZH3/ZH3}$ epileptic crises tended to be longer (but not statistically significantly) than those suffered by *Prnp*$^{+/+}$ mice (*Prnp*$^{+/+}$ = 12.08 ± 3.3 sec; *Prnp*$^{ZH3/ZH3}$ = 19.55 ± 2.5 sec, mean ± S.E.M., $p = 0.12$; Mann-Whitney Test). We postulate that this exacerbated excitability in *Prnp*$^{ZH3/ZH3}$ synapse impaired a proper LTP generation. The HFS may bring about an aberrant synaptic activation (even generating epileptic seizures) that enables activation of the molecular mechanisms needed for LTP induction. Therefore, as published with chemoconvulsants models (Carulla *et al.*, 2015; Walz *et al.*, 1999), PrP^{C} might exert protection against electrically-induced epilepsy.

To gain insight into the gene expression patterns altered in the *Prnp*$^{ZH3/ZH3}$ mice, RNA-seq was performed from the hippocampus region of 8 *Prnp*$^{+/+}$ and 8 *Prnp*$^{ZH3/ZH3}$ animals, revealing only moderate alterations in gene expression profiles (Supplementary Figure 4). According to pathway analysis, the main alterations were the down-regulation of genes associated with the neuronal system (*p*adj. = 6.61 x 10^{-6}) and protein-protein interaction at synapses (*p*adj. = 9.29 x 10^{-6}) (Supplementary Figure 4). Among these, we validated by RT-qPCR some genes that could explain the phenotype shown by the *Prnp*$^{ZH3/ZH3}$ mice: the downregulation of glutamate ionotropic receptor NMDA type subunit 2B (*Grin2b*), the Gamma-Aminobutyric Acid Type A Receptor Subunit Rho2 (*Gabrr2*), the Potassium Voltage-Gated Channels: Subfamily J Member 2 (*Kcnj2*) and 6 (*Kcnj6*), Subfamily A Member 1 (*Kcna1*), and Subfamily Q member 3 (*Kcnq3*)(Supplementary Figure 4).

Enhanced susceptibility to KA-induced seizures in *Prnp*$^{ZH3/ZH3}$ mice correlates with neuronal death in the hippocampus

Next, we aimed to explore whether the absence of PrP^C in the *Prnp*$^{ZH3/ZH3}$ mice increased their susceptibility to epileptic seizures following KA (i.p.) injections, as reported in *Prnp*$^{ZH1/ZH1}$ mice (B6129 and B6.129 backgrounds) (Carulla *et al.*, 2015) (Figure 5). All experiments were carried out on a blind basis, and two different researchers carried out data evaluation (see Material and methods). Three consecutive injections of KA (10 mg/Kg b.w.) were administrated at intervals of 30 min. The epileptic behavior was monitored for 3 h and was categorized into six stages according to its severity (Figure 5A). Results indicate that 67% of *Prnp*$^{+/+}$ mice did not suffer any severe epileptic episodes (stage I-IV). Only 22% and 11% of wild-type mice arrived at stage V and VI, respectively. In contrast, 55% of *Prnp*$^{ZH3/ZH3}$ mice suffered severe epileptic episodes, 20% arriving at stage V and 35% at stage VI (Figure 5A and Supplementary Movie 1). Moreover, *Prnp*$^{ZH3/ZH3}$ mice presented more seizures and blinking episodes per animal than *Prnp*$^{+/+}$ individuals (Seizure: *Prnp*$^{ZH3/ZH3}$ = 2.45 ± 0.74 *vs.* *Prnp*$^{+/+}$ = 1.06 ± 0.83; p = 0.019; Blinking: *Prnp*$^{ZH3/ZH3}$ = 0.95 ± 0.29 *vs.* *Prnp*$^{+/+}$ = 0.22 ± 0.13; mean ± S.E.M. p = 0.069; Mann-Whitney test) (Figure 5B).

Additionally, we evaluated neuronal damage after KA-induced epilepsy with Fluoro-Jade B (Figure 5C-H). *Prnp*$^{ZH3/ZH3}$ mice showed relevant numbers of labeled cells in the pyramidal layer of the CA1-3 (Figure 5C-E), while no signal was observed in *Prnp*$^{+/+}$ sections (Figure 5F-H). These results corroborated the absence of *Prnp* generate an exacerbated synaptic excitability in the hippocampal region that increases susceptibility to electrical and KA-induced seizures, causing neuronal death in the pyramidal layer of the hippocampus proper.

Neuronal *Prnp*$^{ZH3/ZH3}$-derived cultures show reduced bursting and impairment network formation *in vitro*

PrP^{C} has been described as a regulator of neurogenesis and neuronal differentiation *in vitro* and *in vivo* (see Introduction). Moreover, defects in neuronal network connectivity and maturation are related to epilepsy (Stafstrom and Carmant, 2015). Consequently, we tested whether *Prnp*$^{ZH3/ZH3}$ increased excitability might be due to changes in the neuronal differentiation inducing aberrant connectivity and an immature neuronal network. To analyze this, calcium imaging was performed in primary cortical cultures (n = 10 in both genotypes) from *Prnp*$^{+/+}$ and *Prnp*$^{ZH3/ZH3}$ mouse embryos (E16.5-E17.5) expressing the GECI indicator GCaMP6f under the neuronal syntaxin promoter (Chen *et al.*, 2013), allowing us to record calcium traces of the same neuronal population after 8, 11, 13, and 15 days *in vitro* (DIV) (Figure 6A).

Prnp$^{+/+}$ and *Prnp*$^{ZH3/ZH3}$ cultures displayed the same number of collective bursts/min at 8 and 11 DIV (Figure 6B). After that, a delay in *Prnp*$^{ZH3/ZH3}$ neuron activity was observed compared to controls. *Prnp*$^{+/+}$ cultures increased the number of bursts/min significantly at 13 DIV; however, *Prnp*$^{ZH3/ZH3}$ cultures needed two additional days, at 15 DIV (Figure 6A-B). Moreover, *Prnp*$^{+/+}$ neurons exhibited significantly more bursts/min at 13 DIV and 15 DIV than *Prnp*$^{ZH3/ZH3}$ ones and overall the latter showed a reduced firing interval along development (8 Div: *Prnp*$^{+/+}$ = 0.62 ± 0.4 *vs.* *Prnp*$^{ZH3/ZH3}$ = 0.16 ± 0.1 bursts/min; 13 Div: *Prnp*$^{+/+}$ = 4.86 ± 1.1 *vs.* *Prnp*$^{ZH3/ZH3}$ = 1.38 ± 0.4; ***$p < 0.001$; 15 Div: *Prnp*$^{+/+}$ = 9.30 ± 0.7 *vs.* *Prnp*$^{ZH3/ZH3}$ = 5.46 ± 0.4; mean ± S.E.M. ***$p < 0.001$; ANOVA + Bonferroni's multiple comparisons test). The *Prnp*$^{ZH3/ZH3}$ cultures also showed a reduction in

the size of synchronous bursts (Figure 6C). In the *Prnp*$^{+/+}$ cultures, around 80% of the neurons showed synchronic activity at 11, 13, and 15 DIV, while this value was around 50% in *Prnp*$^{ZH3/ZH3}$ cultures (Figure 6C). These results demonstrate that collective bursting is reduced and delayed in *Prnp*$^{ZH3/ZH3}$ cultures, and suggest that *Prnp* expression is necessary for network formation and maturation.

Discussion

PrP^C has been associated with several physiological functions using *in vivo* approaches; however, the consequences of PrP^C deletion in behavior and cognition have not been extensively evaluated (Wulf *et al.*, 2017). There are some studies about *Prnp*$^{0/0}$ mouse behavior, motor capabilities, and learning performance, but the results are not conclusive, especially after the description of the so-called FG in the background of the *Prnp*$^{ZH1/ZH1}$ model that masks specific PrP^C roles (Nuvolone *et al.*, 2013). For example, concerning KA susceptibility, a clear decrease is observed in mice expressing a lower percentage of 129/Sv-associated polymorphisms (B6.129) compared to the B6129 original strain of the *Prnp*$^{ZH1/ZH1}$ mice with a higher percentageof 129/Sv genome (Carulla *et al.*, 2015). Here we assess the consequences of the absence of PrP^C in behavior and neurotransmission using the new strickly co-isogenic mouse model *Prnp*$^{ZH3/ZH3}$ (Nuvolone *et al.*, 2016). However, another relevant aspect of these studies is the age of the analyzed mice, since physiological differences in the absence of *Prnp* have been described in association with age for *Prnp*$^{ZH1/ZH1}$ (Schmitz *et al.*, 2014b) or FVB/N-*Prnp*$^{ZH1/ZH1}$ (Nazor *et al.*, 2007). Thus, in our study, we only used and compared results obtained from mice of 3-5 months of age. Concerning nest-building behavior, our results suggest similar behavior in *Prnp*$^{ZH3/ZH3}$ and wild-type mice. This contrasts with previously reported results (Schmitz *et al.*, 2014b), but it has been largely demonstrated that this capacity is dependent on mouse background (see, e.g. (Bult and Lynch, 1997; Gaskill *et al.*, 2013)).

Our results also reveal that *Prnp*$^{ZH3/ZH3}$ mice display reduced motility in the open field test. The reduced rearing exploration and peripheral preference in the arena,

and the high defecation rate observed in *Prnp*$^{ZH3/ZH3}$ mice, suggest an anxiety-like behavior. Indeed, *Prnp*$^{ZH3/ZH3}$ showed higher thigmotaxis than wild-type mice (see (Simon *et al.*, 1994) for technical details). Our data correlate with those reported by Schmitz *et al.* with *Prnp*$^{ZH1/ZH1}$ mice (Schmitz *et al.*, 2014b) and Lobao-Soares, both using 3-month-old *Prnp*$^{ZH1/ZH1}$ mice, illustrating reduced mobility between the inner and outer regions of the open field and increased defecation in *Prnp*$^{ZH1/ZH1}$ mice (Lobao-Soares *et al.*, 2007). However, they are in contrast to Nico *et al.*, (Nico *et al.*, 2005), where they found no differences, and with Gadotti *et al.* (Gadotti *et al.*, 2012), that showed ten-week-old *Prnp*$^{ZH1/ZH1}$ mice displayed increased crossing in open-field test although thigmotaxis changes were not analyzed in the study. Although technical details could also play a role (i.e., handling of the mice, the initial position of the mice in the field, geometry of the field, etc.), we think that these discrepancies reinforce the relevance of the homogenous genetic background in our study *vs.* the others. In fact, the differences also extend to other tests developed in the same publications: i.e., the rota-rod test, which decreased after 3 min (Nazor *et al.*, 2007), after 5 min (Lobao-Soares *et al.*, 2007), and with no changes at 3 months (Schmitz *et al.*, 2014b).

In our experiments, *Prnp*$^{ZH3/ZH3}$ mice also failed to achieve instrumental learning in the Skinner box. and similar resultswere observed in *Prnp*$^{ZH1/ZH1}$ mice (B6.129 background, 2-5 % 129/Sv markers, (Carulla *et al.*, 2015)). Striking differences in motility between wild-type and knock-out mice were identified using this approach. However, learning capacity based on the ON/OFF paradigm confirmed the operant conditioning deficiencies, a type of associative learning.

Following our results, alterations in locomotor activity and increased latency to initiate exploration were previously reported in other *Prnp*$^{0/0}$ mouse models (Coitinho *et al.*, 2003; Criado *et al.*, 2005). Anxiety-related behavior (Schmitz *et al.*, 2014c), depressive tendencies (Gadotti *et al.*, 2012), and alterations in spatial memory and learning have also been described (Criado *et al.*, 2005; Schmitz *et al.*, 2014a). In contrast, Bueler *et al.* reported no alterations in *Prnp*$^{ZH1/ZH1}$ behavior (Bueler *et al.*, 1992). This disparity in results might be explained by the age of the animals used in the studies. Bueler and collaborators performed the test with 2- and 3-month-old mice, which could potentially uncover the behavior impairment as it was reported to be an age-dependent decline in other publications using the ZH1 model (Rial *et al.*, 2009; Schmitz *et al.*, 2014a). Another study also showed no deficits in *Prnp*$^{0/0}$ mouse behavior, where *Prnp* was conditionally deleted at 12 or 16 months, and the results included no alterations in the Morris water maze or object recognition test (Salazar *et al.*, 2017). We reported behavioral deficits in *Prnp*$^{0/0}$ mouse models with some discrepancies with the previous works, most likely related to age-related sampling and the mice's background.

Glutamate neurotransmission is, in large part, responsible for cortical signaling, and its impairment has been related to behavioral deficits (Russo and Nestler, 2013). PrP^{C} has been described as a regulator of glutamate synapses (Watts *et al.*, 2018). Even glutamate inhibition with an NMDA antagonist (MK-801) ameliorates depressive-like behavior in *Prnp*$^{0/0}$ mice (Gadotti *et al.*, 2012). Thus, our next step was to study glutamate connectivity to better understand behavioral alterations. The hippocampal Schaffer collaterals and their implication in operant

conditioning, spatial learning, and anxiety-related behavior were evaluated as a well-defined model of glutamate circuitry (Anacker and Hen, 2017).

The paired-pulse facilitation test did not show differences between *Prnp*$^{ZH3/ZH3}$ and *Prnp*$^{+/+}$ animals. Therefore, PrP^{C} deletion did not alter synaptic facilitation, at least in the living behaving mouse model. These results may be explained by the fact that synaptic facilitation is mainly a presynaptic phenomenon (Jackman and Regehr, 2017), and PrP^{C} has been related to postsynaptic neurotransmission mechanisms (Carulla *et al.*, 2011; Khosravani *et al.*, 2008).

However, *Prnp*$^{ZH3/ZH3}$ Schaffer collaterals displayed increased excitability at high intensities in the input/output curves test, correlating with increased susceptibility to KA-induced seizures. This epileptogenic phenotype may explain our results on anxiety behavior in *Prnp*$^{ZH3/ZH3}$ mice. Comorbid anxiety disorders affect patients with epilepsy (Kanner, 2011), and cognitive decline has been described in epileptic animal models (Medel-Matus *et al.*, 2017). Moreover, increased excitability was previously reported, especially in susceptibility to KA, NMDA, and pentylenetetrazol (PTZ) insults (i.e., (Rangel *et al.*, 2007; Walz *et al.*, 1999)). Aberrant lateral and collateral branching in the hippocampus's mossy fibers, a phenotype characteristic of epileptic models, has been reported in *Prnp*$^{0/0}$ mice (Colling *et al.*, 1997).

However, contradictory results were published by other groups, who described an elevated epileptic threshold in *Prnp*$^{0/0}$ hippocampal slices treated with bicuculline, zero-magnesium conditions, and PTZ (Ratte *et al.*, 2011), and also normal neurotransmission-associated parameters compared with wild-type mice (Lledo *et al.*, 1996). Both studies recorded hippocampal slices of the FVB/N-

Prnp$^{0/0}$ model, a mouse with a triple mixture background (FVB/129Sv/C57BL6) which carried the FG (Nuvolone *et al.*, 2013). Different susceptibility to KA-induced seizures among mice with different backgrounds has been described; even the FVB background has been shown as highly susceptible to epilepsy (McKhann *et al.*, 2003; Royle *et al.*, 1999). Furthermore, our group described the implication of genetic backgrounds and the FG to KA-induced epilepsy in different *Prnp*$^{0/0}$ mouse models (Carulla *et al.*, 2015). Our results using *Prnp*$^{ZH3/ZH3}$ animals in KA susceptibility were similar to those previously obtained with the other available *Prnp*$^{0/0}$ co-isogenic mouse model, the Edinburgh 129/Ola (Carulla *et al.*, 2015). Therefore, we postulate that these contradictory results published about the excitability of *Prnp*$^{0/0}$ synapse are likely associated with the mouse backgrounds, the FG effect, and the experimental approach. However, the ZH3 mice results demonstrate that PrP^{C} indeed protects against KA-induced epilepsy.

Our results show that the presentation of HFS protocols causes epileptic seizures in most *Prnp*$^{ZH3/ZH3}$ mice but fails to generate significant LTP at the hippocampus. Some controversial results have been published about the implication of PrP^{C} in LTP generation. Different experimental approaches (hippocampal slices or *in vivo* experiments) and a mixture of mouse models with distinct backgrounds were used, generating non-comparable data (i.e., (Collinge *et al.*, 1994; Criado *et al.*, 2005; Lledo *et al.*, 1996; Rangel *et al.*, 2009)). Here, using ZH3 mice, we hypothesize that the absence of PrP^{C} ends in LTP induction failure due to exacerbated synaptic excitability, although we cannot rule out putative GABAergic disinhibition. It is convincingly demonstrated that severe epileptic seizures cause neuronal death, which hampers LTP generation. Moreover, non-severe epileptic seizures generate similar molecular and synaptic changes to

LTP (Meador, 2007; Reid and Stewart, 1997). This suggests that non-severe HFS-induced seizures somehow saturate the postsynaptic terminal, over-activating LTP-induction mechanisms that reduce LTP production capacity by HFS. Additionally, PrP^C has also been described as interacting with key proteins required for LTP-related mechanisms such as PSD-95 (Carulla *et al.*, 2011) and AMPA or NMDA receptors (e.g., (Ferreira *et al.*, 2017; Khosravani *et al.*, 2008; Watt *et al.*, 2012; You *et al.*, 2012)).

The presented data show that $Prnp^{0/0}$ hippocampal synapse is highly excitable and epileptogenic. Alterations in brain connectivity due to developmental alterations, traumas, or infections contribute to this neuromodulation imbalance (Stafstrom and Carmant, 2015). In order to assess whether the epileptic phenotype displayed by $Prnp^{ZH3/ZH3}$ animals came from neuronal connectivity alterations, we studied bursting and network formation in $Prnp^{ZH3/ZH3}$-derived primary neuronal cultures. Relevant PrP^C expression *in vitro* is observed from 4-5 DIV (Gavin *et al.*, 2008). Our results indicate that $Prnp^{ZH3/ZH3}$ cultures did not mature or connect properly; they displayed asynchronous and very low bursting compared to wild-type cultures. These results suggest that the absence of PrP^C causes a delay in neuronal maturation, but more relevantly in neural network formation and function. In fact, the role of PrP^C-mediated signals in neuritogenesis has been demonstrated (i.e., (Amin *et al.*, 2016; Loubet *et al.*, 2012; Pantera *et al.*, 2009). However, to our knowledge, this is the first description of network alterations due to the absence of PrP^C.

Finally, the gene ontology analysis of the RNAseq of $Prnp^{ZH3/ZH3}$ and $Prnp^{+/+}$ mouse hippocampus showed down-regulation of genes associated with the

neuronal system and protein-protein interaction at synapses, fitting the phenotype we observed in the knock-out mice. The significant downregulation of *Gabrr2* and *Grin2b* in *Prnp*$^{ZH3/ZH3}$ mice would produce dysregulation in the excitatory/inhibitory balance, increasing the excitability of the system, as we describe with the KA and the HFS analyses. The alteration of the inhibitory neurotransmission was already shown in *Prnp*$^{0/0}$ models since they were susceptible to suffering from epileptic crises (see references above). PrP^{C} has been widely described as a regulator of glutamatergic neurotransmission and its receptors, as we show here with the *Grin2b*. Moreover, mutations at *Grin2b* have recently been related to a rare brain disease, the *GRIN2B*-related neurodevelopmental disorder that causes intellectual disability, autism-spectrum-like behavior, epilepsy, and, sometimes, locomotor deficiencies as well (Platzer and Lemke, 1993; Platzer *et al.*, 2017). Therefore, the altered expression of *Grin2b* might explain the behavior and learning deficits we observed in our *Prnp*$^{ZH3/ZH3}$ mice.

Increased knowledge of the roles of PrP^{C} in physiology is critical to improve understanding of prionopathy pathophysiology beyond the misfolding and PrP^{Sc} accumulation. Our work characterizes the effects of *Prnp* deletion on behavior, learning, and neurotransmission in the *Prnp*$^{ZH3/ZH3}$ mice. The absence of PrP^{C} impairs neuronal network formation and connectivity, producing enhanced susceptibility to excitotoxicity insults such as HFS and KA exposure. This epileptogenic circuitry seems to impair highly cognitive-demanding functions such as associative learning, and it produces anxiety-like behavior.

Acknowledgments

The authors thank Tom Yohannan for editorial advice and Miriam Segura-Feliu, María Sánchez-Enciso, and José M. González-Martín for their technical help. This research was supported by *PRPSEM* Project with ref. RTI2018-099773-B-I00 from the Spanish Ministry of Science, Innovation, and Universities (MCIU/FEDER/AEI), the CERCA Programme, and the Commission for Universities and Research of the Department of Innovation, Universities, and Enterprise of the Generalitat de Catalunya (SGR2017-648), CIBERNED (CMED2018-2) to JADR. The project leading to these results received funding from the "la Caixa" Foundation (ID 100010434) under the agreement LCF/PR/HR19/52160007 and the María de Maeztu Unit of Excellence (Institute of Neurosciences, University of Barcelona) MDM-2017-0729 to JADR. JS was supported by FIS2016-78507-C2-2-P from (MCIU/FEDER/AEI), SGR2017-1061 from the Generalitat de Catalunya, and the European Union's Horizon 2020 research and innovation program under the grant agreement No. 713140 (MESOBRAIN). Support was also received from MINECO (BFU2017-82375-R), and Junta de Andalucía (BIO-122, UPO-1250734, and P18-FR-823) grants to AG and JMDG. F.L. was supported by Instituto Carlos III (grant PI19-00144). A.M-A. was supported by the Tatiana Pérez de Guzmán el Bueno Foundation.

Figure Legends

Figure 1

Prnp$^{ZH3/ZH3}$ mice show reduced activity and anxiety-related behavior. ***A***, Representative images of *Prnp*$^{+/+}$ and *Prnp*$^{ZH3/ZH3}$ mouse exploratory behavior in the open field test. The dotted line delineates the center and the periphery of the arena. ***B***, Mouse activity in the open field test represented as the number of lines crossed in the X+Y axis. ***C***, Time spent (s) by the mice in the center and periphery of the open field arena. ***D***, Number of rearing and immobility episodes displayed by *Prnp*$^{+/+}$ and *Prnp*$^{ZH3/ZH3}$ mice during the open field test. Data are presented as mean ± S.E.M. $^{**}p < 0.01$ and $^{***}p < 0.001$.

Figure 2

Impairments in the acquisition of an instrumental learning task in *Prnp*$^{ZH3/ZH3}$ mice. ***A***, Percentage of mice reaching the selected criterion (to collect ≥ 20 food pellets for two consecutive days) in the successive training sessions. ***B***, Lever presses of *Prnp*$^{+/+}$ and *Prnp*$^{ZH3/ZH3}$ mice during the fixed ratio (1:1) conditioning paradigm. The test was performed daily for seven consecutive days. ***C***-***D***, Lever presses of *Prnp*$^{+/+}$ (***C***) and *Prnp*$^{ZH3/ZH3}$ (***D***) mice during the ON/OFF training paradigm. Lines represent best linear fits for lever presses evoked during light ON (grey) and light OFF (black) periods. Equations corresponding to regression lines are illustrated in **C** and **D**, including R^2 coefficients. Data are presented as a percentage in ***A***, and as mean ± S.E.M. in ***B***, ***C*** and ***D***. $^{**}p < 0.01$ and $^{***}p < 0.001$.

Figure 3

CA3-CA1 synapses in *Prnp*$^{ZH3/ZH3}$ mice show enhanced excitability. ***A***, Schematic representation of electrodes implanted in mouse dorsal hippocampus. Two stimulation electrodes are implanted in the Schaffer collateral pathway in the CA3 region and two recording electrodes in the CA1 *stratum radiatum*. ***B***, Effects of the paired-pulse stimulation of the Schaffer collateral pathway at increasing inter-stimulus intervals (10, 20, 40, 100, 200, 500 ms). Data are presented as the percentage of increase of fEPSP2 in relation to fEPSP1 (fEPSP2/fEPSP1 * 100). ***C***-***D***, Input/output curves of fEPSPs (V/s) in CA1 after the presentation of paired-pulses of increasing intensities in the CA3 area (0.02 mA to 0.4mA) of *Prnp*$^{+/+}$ (***C***) and *Prnp*$^{ZH3/ZH3}$ (***D***) mice. ***E***, Paired pulse ratio (fEPSP2 / fEPSP1 * 100) of data illustrated in ***C*** and ***D***. ***F***, Area under the curve (a.u.) of PP ratio from 0.24 mA to 0.4 intensities. Data are presented as mean ± S.E.M. *$p < 0.05$, **$p < 0.01$, and ***$p < 0.001$.

Figure 4

LTP is not induced at CA3-CA1 synapses of *Prnp*$^{ZH3/ZH3}$ mice, and the HFS presentation generates epileptic seizures. ***A***-***B***, Evolution of fEPSP1 evoked in the CA1 region by paired-pulsed stimulation of Schaffer collaterals for the *Prnp*$^{+/+}$ (***A***) and *Prnp*$^{ZH3/ZH3}$ (***B***) mice after the HFS session. Data are presented as the percentage of increase from baseline. Significant differences with baseline values are presented for fEPSP1 (*) and fEPSP2 (#) recordings in *Prnp*$^{+/+}$ mice. ***C***-***D***, fEPSP mean slopes from *Prnp*$^{+/+}$ (***C***), and *Prnp*$^{ZH3/ZH3}$ (***D***) mice before and after the HFS session. Data are presented as the percentage of increase from baseline values. ***E***, Representative examples of long (30 s) recordings carried out after an

HFS stimulation protocol in *Prnp*$^{+/+}$ and *Prnp*$^{ZH3/ZH3}$ Schaffer collaterals. Note the presence of a hippocampal seizure in the *Prnp*$^{ZH3/ZH3}$ mouse (arrows). ***F***, Percentage of mice that presented epileptic seizures following HFS presentations. ***G***, Seizure duration (s) following HFS. Data are presented as Mean ± S.E.M. *$p < 0.05$, **$p < 0.01$, ***$p < 0.001$, $^{\#\#}p < 0.01$ and $^{\#\#}p < 0.001$.

Figure 5

Prnp$^{ZH3/ZH3}$ mice are more susceptible to kainate-induced epilepsy correlating with increased neuronal death in CA1 and CA3 pyramidal layers. ***A***, Percentage of mice reaching stage I-IV, V, or VI epileptic phenotype after KA administration (10 mg/Kg). ***B***, Number of seizures and blinking episodes presented by *Prnp*$^{+/+}$ and *Prnp*$^{ZH3/ZH3}$ mice for 3 h after KA administration. ***C-H***, Photomicrographs showing the pattern of neurodegeneration with Fluoro-Jade B staining seven days after KA treatment in *Prnp*$^{+/+}$ (**C**-**E**) and *Prnp*$^{ZH3/ZH3}$ (**F-H**) mouse hippocampus. Nuclei are stained with DAPI (**C**, **F**). Dying cells (**D**, **G**, stained with Fluoro-Jade B) are located in the pyramidal cell layer of CA1 (arrow) and CA3 (arrowhead) areas. Data are presented as a percentage in ***A*** and as mean ± S.E.M. in ***B***. Abbreviations: so, *stratum oriens*; sp, *stratum pyramidale*; sr, *stratum radiatum*; slm, *stratum lacunosum-moleculare*; DG, dentate gyrus. Scale bar represents 500 µm. *$p < 0.05$.

Figure 6

Reduced bursting and network formation in neuronal *Prnp*$^{ZH3/ZH3}$-derived cultures. ***A***, Representative examples of neuronal traces at 8 and 15 DIV in the *Prnp*$^{+/+}$ and *Prnp*$^{ZH3/ZH3}$ primary cultures. Note the asynchrony in the *Prnp*$^{ZH3/ZH3}$ culture. ***B***, Evolution of network bursting in *Prnp*$^{+/+}$ and *Prnp*$^{ZH3/ZH3}$ neuronal

cultures from 8 to 15 DIV. Data are presented as the mean of bursts/min ± S.E.M. ***C***, Evolution of size of synchronous bursts from 8 to 15 DIV. Data are presented as the mean percentage of active neurons ± S.E.M. Asterisks (*) indicate significant differences between *Prnp*$^{+/+}$ and *Prnp*$^{ZH3/ZH3}$ bursting. Number sign (#) indicates significant differences with the respective baseline bursting at 8 DIV. *$p < 0.05$, ***$p < 0.001$ and $^{\#\#\#}p < 0.001$.

Supplementary information

Supplementary Figure 1

Prnp$^{ZH3/ZH3}$ mice showed similar nest-building behavior to wild-type mice. ***A***, Representative images of nests constructed by *Prnp*$^{+/+}$ (left) and *Prnp*$^{ZH3/ZH3}$ mice (right). ***B***, Quantification illustrating the mean of the nest score (see Material and methods for details). Although a tendency can be seen, no significant differences are observed. Data are presented as mean ± S.E.M.

Supplementary Figure 2

Prnp$^{ZH1/ZH1}$ mice failed to acquire an instrumental learning test using a fixed ratio (1:1) schedule. ***A***, Percentage of *Prnp*$^{+/+}$ and *Prnp*$^{ZH1/ZH1}$ mice reached the selected criterion during the training sessions. ***B***, Task accuracy ((lever presses during light ON – lever presses during the light OFF)/Total number of lever presses) during the light ON/light OFF conditioning paradigm. In contrast to control mice, knock-out mice did present a sustained increase in their scores. Data are presented as a percentage in ***A*** and as mean ± S.E.M. in ***B***.

Supplementary Figure 3

Stressed-like behavior in *Prnp*$^{ZH3/ZH3}$ mice impairing object recognition test performance. *Prnp*$^{ZH1/ZH1}$ mice also showed stressed-like behavior and failed to acquire short-term memory. ***A***, Scheme of object recognition protocol. This consisted of 3 sessions (10 min each). First, mice were habituated in the empty arena. One hour later, they were placed again in the arena with two identical objects for the training session. Finally, 2-3 h later, they were once more placed in the arena, replacing one object with a novel one for the short-term memory test. Fecal bodies (*Prnp*$^{ZH3/ZH3}$) and rearing episodes (*Prnp*$^{ZH1/ZH1}$) were counted in the habituation session as an indicator of animal stress. ***B***, Number of fecal bodies generated per animal (*Prnp*$^{+/+}$ and *Prnp*$^{ZH3/ZH3}$) during the habituation session. Data are presented as mean ± S.E.M. ***C***-***D*** Time that *Prnp*$^{+/+}$ (***C***), and *Prnp*$^{ZH3/ZH3}$ (***D***) mice interacted with the objects in the short-term test. Data are presented as the percentage of mice interacting with the object in each time interval (0 to 35 s). ***E***, Number of rearing episodes in the habituation session (*Prnp*$^{+/+}$ and *Prnp*$^{ZH1/ZH1}$). ***F***-***G***, Relative time that the two exposed objects are explored to the total time invested. Object 1 (O_1) and object 1' (O_1') in the training session (***F***) and number, and object 1 (O_1) and object 2 (O_2) in the short-term memory test (***G***). Data are presented as a percentage in ***C***-***D*** and as mean ± S.E.M. in ***B***, ***E***, ***F***, ***G***. *$p < 0.05$ and ***$p < 0.001$.

Supplementary Figure 4

Gene ontology analysis of RNAseq from the *Prnp*$^{ZH3/ZH3}$ hippocampus showing dysregulation of neuronal and synaptic pathways. ***A***, Table of significantly downregulated and upregulated gene pathways. Validation of the main genes

altered by RT-qPCR: *Grin2b* (***B***), *Gabrr2* (***C***), *Kcnj6* (***D***), *Kcna1* (***E***), *Kcnj2* (***F***), and *Kcnq3* (***G***). Data are presented as mean ± S.E.M. *$p < 0.05$ and ***$p < 0.001$.

Supplementary Movie 1

Representative movie of *Prnp*$^{+/+}$ (bottom and up-left) and *Prnp*$^{ZH3/ZH3}$ (middle and up-right) mouse behavior after KA (middle and bottom) and PBS (top) administration. Note the blinking and seizure episodes suffered by the *Prnp*$^{ZH3/ZH3}$ mice treated with KA (labeled with asterisks at the beginning of the video).

REFERENCES

Adao-Novaes, J., Valverde, R.H.F., Landemberger, M.C., Silveira, M.S., Simoes-Pires, E.N., Lowe, J., Linden, R., 2020. Substrain-related dependence of Cu(I)-ATPase activity among prion protein-null mice. *Brain Res* 1727**,** 146550.

Adle-Biassette, H., Verney, C., Peoc'h, K., Dauge, M.C., Razavi, F., Choudat, L., Gressens, P., Budka, H., Henin, D., 2006. Immunohistochemical expression of prion protein (PrPC) in the human forebrain during development. *J Neuropathol Exp Neurol* 65**,** 698-706.

Aguzzi, A., 2000. Molecular pathology of prion diseases. *Vox Sang* 78 Suppl 2**,** 25.

Amin, L., Nguyen, X.T., Rolle, I.G., D'Este, E., Giachin, G., Tran, T.H., Serbec, V.C., Cojoc, D., Legname, G., 2016. Characterization of prion protein function by focal neurite stimulation. *J Cell Sci* 129**,** 3878-3891.

Anacker, C., Hen, R., 2017. Adult hippocampal neurogenesis and cognitive flexibility — linking memory and mood. *Nature Reviews Neuroscience* 18**,** 335.

Baldwin, K.J., Correll, C.M., 2019. Prion Disease. *Semin Neurol* 39**,** 428-439.

Bribian, A., Fontana, X., Llorens, F., Gavin, R., Reina, M., Garcia-Verdugo, J.M., Torres, J.M., de Castro, F., del Rio, J.A., 2012. Role of the cellular prion protein in oligodendrocyte precursor cell proliferation and differentiation in the developing and adult mouse CNS. *PLoS One* 7**,** e33872.

Brown, E.J., Frazier, W.A., 2001. Integrin-associated protein (CD47) and its ligands. *Trends Cell Biol* 11**,** 130-135.

Bueler, H., Fischer, M., Lang, Y., Bluethmann, H., Lipp, H.P., DeArmond, S.J., Prusiner, S.B., Aguet, M., Weissmann, C., 1992. Normal development and behaviour of mice lacking the neuronal cell-surface PrP protein. *Nature* 356**,** 577-582.

Bult, A., Lynch, C.B., 1997. Nesting and fitness: lifetime reproductive success in house mice bidirectionally selected for thermoregulatory nest-building behavior. *Behav Genet* 27**,** 231-240.

Carulla, P., Bribian, A., Rangel, A., Gavin, R., Ferrer, I., Caelles, C., Del Rio, J.A., Llorens, F., 2011. Neuroprotective role of PrPC against kainate-induced epileptic seizures and cell death depends on the modulation of JNK3 activation by GluR6/7-PSD-95 binding. *Mol Biol Cell* 22**,** 3041-3054.

Carulla, P., Llorens, F., Matamoros-Angles, A., Aguilar-Calvo, P., Espinosa, J.C., Gavin, R., Ferrer, I., Legname, G., Torres, J.M., del Rio, J.A., 2015. Involvement of PrP(C) in kainate-induced excitotoxicity in several mouse strains. *Sci Rep* 5**,** 11971.

Chen, T.W., Wardill, T.J., Sun, Y., Pulver, S.R., Renninger, S.L., Baohan, A., Schreiter, E.R., Kerr, R.A., Orger, M.B., Jayaraman, V., Looger, L.L., Svoboda, K., Kim, D.S., 2013. Ultrasensitive fluorescent proteins for imaging neuronal activity. *Nature* 499**,** 295-300.

Chiarini, L.B., Freitas, A.R., Zanata, S.M., Brentani, R.R., Martins, V.R., Linden, R., 2002. Cellular prion protein transduces neuroprotective signals. *EMBO J* 21**,** 3317-3326.

Clarke, J.R., Cammarota, M., Gruart, A., Izquierdo, I., Delgado-García, J.M. 2010. Plastic modifications induced by object recognition memory processing. In: *Proc Natl Acad Sci U S A* 107, 2652-2657.

Coitinho, A.S., Roesler, R., Martins, V.R., Brentani, R.R., Izquierdo, I., 2003. Cellular prion protein ablation impairs behavior as a function of age. *Neuroreport* 14**,** 1375-1379.

Colling, S.B., Khana, M., Collinge, J., Jefferys, J.G., 1997. Mossy fibre reorganization in the hippocampus of prion protein null mice. *Brain Res* 755**,** 28-35.

Collinge, J., Whittington, M.A., Sidle, K.C., Smith, C.J., Palmer, M.S., Clarke, A.R., Jefferys, J.G., 1994. Prion protein is necessary for normal synaptic function. *Nature* 370**,** 295-297.

Criado, J.R., Sanchez-Alavez, M., Conti, B., Giacchino, J.L., Wills, D.N., Henriksen, S.J., Race, R., Manson, J.C., Chesebro, B., Oldstone, M.B., 2005. Mice devoid of prion protein have cognitive deficits that are rescued by reconstitution of PrP in neurons. *Neurobiol Dis* 19**,** 255-265.
Curtis, J., Errington, M., Bliss, T., Voss, K., MacLeod, N., 2003. Age-dependent loss of PTP and LTP in the hippocampus of PrP-null mice. *Neurobiol Dis* 13**,** 55-62.
de Almeida, C.J., Chiarini, L.B., da Silva, J.P., PM, E.S., Martins, M.A., Linden, R., 2005. The cellular prion protein modulates phagocytosis and inflammatory response. *J Leukoc Biol* 77**,** 238-246.
Deacon, R.M., 2006. Assessing nest building in mice. *Nat Protoc* 1**,** 1117-1119.
Del Rio, J.A., Ferrer, I., Gavin, R., 2018. Role of cellular prion protein in interneuronal amyloid transmission. *Prog Neurobiol* 165-167**,** 87-102.
del Rio, J.A., Gavin, R., 2016. Functions of the cellular prion protein, the end of Moore's law, and Ockham's razor theory. *Prion* 10**,** 25-40.
Dobin, A., Davis, C.A., Schlesinger, F., Drenkow, J., Zaleski, C., Jha, S., Batut, P., Chaisson, M., Gingeras, T.R., 2013. STAR: ultrafast universal RNA-seq aligner. *Bioinformatics* 29**,** 15-21.
Encalada, S.E., Szpankowski, L., Xia, C.H., Goldstein, L.S., 2011. Stable kinesin and dynein assemblies drive the axonal transport of mammalian prion protein vesicles. *Cell* 144**,** 551-565.
Fainstein, N., Dori, D., Frid, K., Fritz, A.T., Shapiro, I., Gabizon, R., Ben-Hur, T., 2016. Chronic progressive neurodegeneration in a transgenic mouse model of prion disease. *Front Neurosci* 10**,** 510.
Ferreira, D.G., Temido-Ferreira, M., Vicente Miranda, H., Batalha, V.L., Coelho, J.E., Szego, E.M., Marques-Morgado, I., Vaz, S.H., Rhee, J.S., Schmitz, M., Zerr, I., Lopes, L.V., Outeiro, T.F., 2017. alpha-synuclein interacts with PrP(C) to induce cognitive impairment through mGluR5 and NMDAR2B. *Nat Neurosci* 20**,** 1569-1579.
Fischer, M., Rulicke, T., Raeber, A., Sailer, A., Moser, M., Oesch, B., Brandner, S., Aguzzi, A., Weissmann, C., 1996. Prion protein (PrP) with amino-proximal deletions restoring susceptibility of PrP knockout mice to scrapie. *EMBO J* 15**,** 1255-1264.
Flechsig, E., Hegyi, I., Leimeroth, R., Zuniga, A., Rossi, D., Cozzio, A., Schwarz, P., Rulicke, T., Gotz, J., Aguzzi, A., Weissmann, C., 2003. Expression of truncated PrP targeted to Purkinje cells of PrP knockout mice causes Purkinje cell death and ataxia. *EMBO J* 22**,** 3095-3101.
Ford, M.J., Burton, L.J., Morris, R.J., Hall, S.M., 2002. Selective expression of prion protein in peripheral tissues of the adult mouse. *Neuroscience* 113**,** 177-192.
Gadotti, V.M., Bonfield, S.P., Zamponi, G.W., 2012. Depressive-like behaviour of mice lacking cellular prion protein. *Behav Brain Res* 227**,** 319-323.
Gaskill, B.N., Karas, A.Z., Garner, J.P., Pritchett-Corning, K.R., 2013. Nest building as an indicator of health and welfare in laboratory mice. *J Vis Exp***,** 51012.
Gavin, R., Lidon, L., Ferrer, I., Del Rio, J.A., 2020. The quest for cellular prion protein functions in the aged and neurodegenerating brain. *Cells* 9.
Gavin, R., Urena, J., Rangel, A., Pastrana, M.A., Requena, J.R., Soriano, E., Aguzzi, A., Del Rio, J.A., 2008. Fibrillar prion peptide PrP(106-126) treatment induces Dab1 phosphorylation and impairs APP processing and Abeta production in cortical neurons. *Neurobiol Dis* 30**,** 243-254.
Goetzl, E.J., Peltz, C.B., Mustapic, M., Kapogiannis, D., Yaffe, K., 2020. Neuron-derived plasma exosome proteins after remote traumatic brain injury. *J Neurotrauma* 37**,** 382-388.
Griffoni, C., Toni, M., Spisni, E., Bianco, M., Santi, S., Riccio, M., Tomasi, V., 2003. The cellular prion protein: biochemistry, topology, and physiologic functions. *Cell Biochem Biophys* 38**,** 287-304.
Involvement of the CA3-CA1 synapse in the acquisition of associative learning in behaving mice.

Gruart, A., Muñoz, M.D., Delgado-García, J.M., 2006. Involvement of the CA3-CA1 synapse in the acquisition of associative learning in behavind mice. *J Neurosci* 26:1077-1087.
Hara, H., Miyata, H., Das, N.R., Chida, J., Yoshimochi, T., Uchiyama, K., Watanabe, H., Kondoh, G., Yokoyama, T., Sakaguchi, S., 2018. Prion protein devoid of the octapeptide repeat region delays bovine spongiform encephalopathy pathogenesis in mice. *J Virol* 92.
Hasan, M.T., Hernández-González, S., Dogbevia, G., Treviño, M., Bertocchi, I., Gruart, A., Delgado-García, J.M., 2013. Role of motor cortex NMDA receptors in learning-dependent synaptic plasticity of behaving mice. *Nat Commun* 4:2258. doi: 10.1038/ncomms3258.
Huber, W., Carey, V.J., Gentleman, R., Anders, S., Carlson, M., Carvalho, B.S., Bravo, H.C., Davis, S., Gatto, L., Girke, T., Gottardo, R., Hahne, F., Hansen, K.D., Irizarry, R.A., Lawrence, M., Love, M.I., MacDonald, J., Obenchain, V., Oles, A.K., Pages, H., Reyes, A., Shannon, P., Smyth, G.K., Tenenbaum, D., Waldron, L., Morgan, M., 2015. Orchestrating high-throughput genomic analysis with Bioconductor. *Nat Methods* 12**,** 115-121.
Jackman, S.L., Regehr, W.G., 2017. The mechanisms and functions of synaptic facilitation. *Neuron* 94**,** 447-464.
Jang, M.J., Nam, Y., 2015. NeuroCa: integrated framework for systematic analysis of spatiotemporal neuronal activity patterns from large-scale optical recording data. *Neurophotonics* 2**,** 035003.
Jirkof, P., 2014. Burrowing and nest building behavior as indicators of well-being in mice. *J Neurosci Methods* 234**,** 139-146.
Kanner, A.M., 2011. Anxiety disorders in epilepsy: the forgotten psychiatric comorbidity. *Epilepsy Curr* 11**,** 90-91.
Khosravani, H., Zhang, Y., Tsutsui, S., Hameed, S., Altier, C., Hamid, J., Chen, L., Villemaire, M., Ali, Z., Jirik, F.R., Zamponi, G.W., 2008. Prion protein attenuates excitotoxicity by inhibiting NMDA receptors. *J Cell Biol* 181**,** 551-565.
Legname, G., 2017. Elucidating the function of the prion protein. *PLoS Pathog* 13**,** e1006458.
Leng, B., Sun, H., Zhao, J., Liu, Y., Shen, T., Liu, W., Liu, X., Tan, M., Li, F., Zhang, J., Li, Z., 2020. Plasma exosomal prion protein levels are correlated with cognitive decline in PD patients. *Neurosci Lett* 723**,** 134866.
Lidon, L., Vergara, C., Ferrer, I., Hernandez, F., Avila, J., Del Rio, J.A., Gavin, R., 2020. Tau protein as a new regulator of cellular prion protein transcription. *Mol Neurobiol*.
Lima, F.R., Arantes, C.P., Muras, A.G., Nomizo, R., Brentani, R.R., Martins, V.R., 2007. Cellular prion protein expression in astrocytes modulates neuronal survival and differentiation. *J Neurochem* 103**,** 2164-2176.
Linden, R., Martins, V.R., Prado, M.A., Cammarota, M., Izquierdo, I., Brentani, R.R., 2008. Physiology of the prion protein. *Physiol Rev* 88**,** 673-728.
Lipp, H.P., Stagliar-Bozicevic, M., Fischer, M., Wolfer, D.P., 1998. A 2-year longitudinal study of swimming navigation in mice devoid of the prion protein: no evidence for neurological anomalies or spatial learning impairments. *Behav Brain Res* 95**,** 47-54.
Lledo, P.M., Tremblay, P., DeArmond, S.J., Prusiner, S.B., Nicoll, R.A., 1996. Mice deficient for prion protein exhibit normal neuronal excitability and synaptic transmission in the hippocampus. *Proc Natl Acad Sci U S A* 93**,** 2403-2407.
Llorens, F., Ansoleaga, B., Garcia-Esparcia, P., Zafar, S., Grau-Rivera, O., Lopez-Gonzalez, I., Blanco, R., Carmona, M., Yague, J., Nos, C., Del Rio, J.A., Gelpi, E., Zerr, I., Ferrer, I., 2013. PrP mRNA and protein expression in brain and PrP(c) in CSF in Creutzfeldt-Jakob disease MM1 and VV2. *Prion* 7**,** 383-393.
Llorens, F., Del Rio, J.A., 2012. Unraveling the neuroprotective mechanisms of PrP (C) in excitotoxicity. *Prion* 6**,** 245-251.

Lobao-Soares, B., Walz, R., Carlotti, C.G., Jr., Sakamoto, A.C., Calvo, F., Terzian, A.L., da Silva, J.A., Wichert-Ana, L., Coimbra, N.C., Bianchin, M.M., 2007. Cellular prion protein regulates the motor behaviour performance and anxiety-induced responses in genetically modified mice. *Behav Brain Res* 183**,** 87-94.

Loubet, D., Dakowski, C., Pietri, M., Pradines, E., Bernard, S., Callebert, J., Ardila-Osorio, H., Mouillet-Richard, S., Launay, J.M., Kellermann, O., Schneider, B., 2012. Neuritogenesis: the prion protein controls beta1 integrin signaling activity. *FASEB J* 26**,** 678-690.

Love, M.I., Huber, W., Anders, S., 2014. Moderated estimation of fold change and dispersion for RNA-seq data with DESeq2. *Genome Biol* 15**,** 550.

Madroñal, N., López-Aracil, C., Rangel, A., del Rio, J.A., Delgado-García, J.M., Gruart, A., 2010. Effects of enriched physical and social environments on motor performance, associative learning, and hippocampal neurogenesis in mice. *PLoS One* 5**,** e11130.

Madroñal, N., Gruart, A., Delgado-García, J.M., 2009. Differing presynaptic contributions to LTP and associative learning in behaving mice. *Front Behav Neurosci* 3**,** 7.

Maglio, L.E., Martins, V.R., Izquierdo, I., Ramirez, O.A., 2006. Role of cellular prion protein on LTP expression in aged mice. *Brain Res* 1097**,** 11-18.

Manson, J.C., Clarke, A.R., Hooper, M.L., Aitchison, L., McConnell, I., Hope, J., 1994. 129/Ola mice carrying a null mutation in PrP that abolishes mRNA production are developmentally normal. *Mol Neurobiol* 8**,** 121-127.

Manson, J.C., Hope, J., Clarke, A.R., Johnston, A., Black, C., MacLeod, N., 1995. PrP gene dosage and long term potentiation. *Neurodegeneration* 4**,** 113-114.

McKhann, G.M., 2nd, Wenzel, H.J., Robbins, C.A., Sosunov, A.A., Schwartzkroin, P.A., 2003. Mouse strain differences in kainic acid sensitivity, seizure behavior, mortality, and hippocampal pathology. *Neuroscience* 122**,** 551-561.

Meador, K.J., 2007. The basic science of memory as it applies to epilepsy. *Epilepsia* 48 Suppl 9**,** 23-25.

Medel-Matus, J.S., Shin, D., Sankar, R., Mazarati, A., 2017. Kindling epileptogenesis and panic-like behavior: Their bidirectional connection and contribution to epilepsy-associated depression. *Epilepsy Behav* 77**,** 33-38.

Medrano-Fernandez, A., Delgado-Garcia, J.M., Del Blanco, B., Llinares, M., Sanchez-Campusano, R., Olivares, R., Gruart, A., Barco, A., 2018. The epigenetic factor CBP is required for the differentiation and function of medial ganglionic eminence-derived interneurons. *Mol Neurobiol*.

Moser, M., Colello, R.J., Pott, U., Oesch, B., 1995. Developmental expression of the prion protein gene in glial cells. *Neuron* 14**,** 509-517.

Nazor, K.E., Seward, T., Telling, G.C., 2007. Motor behavioral and neuropathological deficits in mice deficient for normal prion protein expression. *Biochim Biophys Acta* 1772**,** 645-653.

Nico, P.B., de-Paris, F., Vinade, E.R., Amaral, O.B., Rockenbach, I., Soares, B.L., Guarnieri, R., Wichert-Ana, L., Calvo, F., Walz, R., Izquierdo, I., Sakamoto, A.C., Brentani, R., Martins, V.R., Bianchin, M.M., 2005. Altered behavioural response to acute stress in mice lacking cellular prion protein. *Behav Brain Res* 162**,** 173-181.

Nicolas, O., Gavin, R., del Rio, J.A., 2009. New insights into cellular prion protein (PrPc) functions: the "ying and yang" of a relevant protein. *Brain Res Rev* 61**,** 170-184.

Nishimura, T., Sakudo, A., Hashiyama, Y., Yachi, A., Saeki, K., Matsumoto, Y., Ogawa, M., Sakaguchi, S., Itohara, S., Onodera, T., 2007. Serum withdrawal-induced apoptosis in ZrchI prion protein (PrP) gene-deficient neuronal cell line is suppressed by PrP, independent of Doppel. *Microbiol Immunol* 51**,** 457-466.

Nuvolone, M., Hermann, M., Sorce, S., Russo, G., Tiberi, C., Schwarz, P., Minikel, E., Sanoudou, D., Pelczar, P., Aguzzi, A., 2016. Strictly co-isogenic C57BL/6J-Prnp-/- mice: A rigorous resource for prion science. *J Exp Med* 213**,** 313-327.

Nuvolone, M., Kana, V., Hutter, G., Sakata, D., Mortin-Toth, S.M., Russo, G., Danska, J.S., Aguzzi, A., 2013. SIRPalpha polymorphisms, but not the prion protein, control phagocytosis of apoptotic cells. *J Exp Med* 210**,** 2539-2552.
Nuvolone, M., Paolucci, M., Sorce, S., Kana, V., Moos, R., Matozaki, T., Aguzzi, A., 2017a. Prion pathogenesis is unaltered in the absence of SIRPalpha-mediated "don't-eat-me" signaling. *PLoS One* 12**,** e0177876.
Nuvolone, M., Sorce, S., Paolucci, M., Aguzzi, A., 2017b. Extended characterization of the novel co-isogenic C57BL/6J Prnp(-/-) mouse line. *Amyloid* 24**,** 36-37.
Onodera, T., Sakudo, A., Tsubone, H., Itohara, S., 2014. Review of studies that have used knockout mice to assess normal function of prion protein under immunological or pathophysiological stress. *Microbiol Immunol* 58**,** 361-374.
Orlandi, J.G., Stetter, O., Soriano, J., Geisel, T., Battaglia, D., 2014. Transfer entropy reconstruction and labeling of neuronal connections from simulated calcium imaging. *PLoS One* 9**,** e98842.
Paitel, E., Fahraeus, R., Checler, F., 2003. Cellular prion protein sensitizes neurons to apoptotic stimuli through Mdm2-regulated and p53-dependent caspase 3-like activation. *The Journal of biological chemistry* 278**,** 10061-10066.
Paitel, E., Sunyach, C., Alves da Costa, C., Bourdon, J.C., Vincent, B., Checler, F., 2004. Primary cultured neurons devoid of cellular prion display lower responsiveness to staurosporine through the control of p53 at both transcriptional and post-transcriptional levels. *J Biol Chem* 279**,** 612-618.
Pantera, B., Bini, C., Cirri, P., Paoli, P., Camici, G., Manao, G., Caselli, A., 2009. PrPc activation induces neurite outgrowth and differentiation in PC12 cells: role for caveolin-1 in the signal transduction pathway. *J Neurochem* 110**,** 194-207.
Platzer, K., Lemke, J.R. 1993. GRIN2B-related neurodevelopmental disorder. In: *GeneReviews((R))*. Eds. M.P. Adam, H.H. Ardinger, R.A. Pagon, S.E. Wallace, L.J.H. Bean, K. Stephens, A. Amemiya: Seattle (WA).
Platzer, K., Yuan, H., Schutz, H., Winschel, A., Chen, W., Hu, C., Kusumoto, H., Heyne, H.O., Helbig, K.L., Tang, S., Willing, M.C., Tinkle, B.T., Adams, D.J., Depienne, C., Keren, B., Mignot, C., Frengen, E., Stromme, P., Biskup, S., Docker, D., Strom, T.M., Mefford, H.C., Myers, C.T., Muir, A.M., LaCroix, A., Sadleir, L., Scheffer, I.E., Brilstra, E., van Haelst, M.M., van der Smagt, J.J., Bok, L.A., Moller, R.S., Jensen, U.B., Millichap, J.J., Berg, A.T., Goldberg, E.M., De Bie, I., Fox, S., Major, P., Jones, J.R., Zackai, E.H., Abou Jamra, R., Rolfs, A., Leventer, R.J., Lawson, J.A., Roscioli, T., Jansen, F.E., Ranza, E., Korff, C.M., Lehesjoki, A.E., Courage, C., Linnankivi, T., Smith, D.R., Stanley, C., Mintz, M., McKnight, D., Decker, A., Tan, W.H., Tarnopolsky, M.A., Brady, L.I., Wolff, M., Dondit, L., Pedro, H.F., Parisotto, S.E., Jones, K.L., Patel, A.D., Franz, D.N., Vanzo, R., Marco, E., Ranells, J.D., Di Donato, N., Dobyns, W.B., Laube, B., Traynelis, S.F., Lemke, J.R., 2017. GRIN2B encephalopathy: novel findings on phenotype, variant clustering, functional consequences and treatment aspects. *J Med Genet* 54**,** 460-470.
Prusiner, S.B., DeArmond, S.J., 1994. Prion diseases and neurodegeneration. *Annu Rev Neurosci* 17**,** 311-339.
Rangel, A., Burgaya, F., Gavin, R., Soriano, E., Aguzzi, A., Del Rio, J.A., 2007. Enhanced susceptibility of Prnp-deficient mice to kainate-induced seizures, neuronal apoptosis, and death: Role of AMPA/kainate receptors. *J Neurosci Res* 85**,** 2741-2755.
Rangel, A., Madronal, N., Gruart, A., Gavin, R., Llorens, F., Sumoy, L., Torres, J.M., Delgado-Garcia, J.M., Del Rio, J.A., 2009. Regulation of GABA(A) and glutamate receptor expression, synaptic facilitation and long-term potentiation in the hippocampus of prion mutant mice. *PLoS One* 4**,** e7592.
Ratte, S., Vreugdenhil, M., Boult, J.K., Patel, A., Asante, E.A., Collinge, J., Jefferys, J.G., 2011. Threshold for epileptiform activity is elevated in prion knockout mice. *Neuroscience* 179**,** 56-61.

Reid, I.C., Stewart, C.A., 1997. Seizures, memory and synaptic plasticity. *Seizure* 6**,** 351-359.
Resenberger, U.K., Winklhofer, K.F., Tatzelt, J., 2011. Neuroprotective and neurotoxic signaling by the prion protein. *Top Curr Chem* 305**,** 101-119.
Rial, D., Duarte, F.S., Xikota, J.C., Schmitz, A.E., Dafre, A.L., Figueiredo, C.P., Walz, R., Prediger, R.D., 2009. Cellular prion protein modulates age-related behavioral and neurochemical alterations in mice. *Neuroscience* 164**,** 896-907.
Roucou, X., Gains, M., LeBlanc, A.C., 2004. Neuroprotective functions of prion protein. *J Neurosci Res* 75**,** 153-161.
Royle, S.J., Collins, F.C., Rupniak, H.T., Barnes, J.C., Anderson, R., 1999. Behavioural analysis and susceptibility to CNS injury of four inbred strains of mice. *Brain Res* 816**,** 337-349.
Russo, S.J., Nestler, E.J., 2013. The brain reward circuitry in mood disorders. *Nature Reviews Neuroscience* 14**,** 609.
Salazar, S.V., Gallardo, C., Kaufman, A.C., Herber, C.S., Haas, L.T., Robinson, S., Manson, J.C., Lee, M.K., Strittmatter, S.M., 2017. Conditional deletion of prnp rescues behavioral and synaptic deficits after disease onset in transgenic Alzheimer's disease. *J Neurosci* 37**,** 9207-9221.
Scalabrino, G., Veber, D., De Giuseppe, R., Roncaroli, F., 2015. Low levels of cobalamin, epidermal growth factor, and normal prions in multiple sclerosis spinal cord. *Neuroscience* 298**,** 293-301.
Schmieder, R., Lim, Y.W., Edwards, R., 2012. Identification and removal of ribosomal RNA sequences from metatranscriptomes. *Bioinformatics* 28**,** 433-435.
Schmitz, M., Greis, C., Ottis, P., Silva, C.J., Schulz-Schaeffer, W.J., Wrede, A., Koppe, K., Onisko, B., Requena, J.R., Govindarajan, N., Korth, C., Fischer, A., Zerr, I., 2014a. Loss of prion protein leads to age-dependent behavioral abnormalities and changes in cytoskeletal protein expression. *Mol Neurobiol*.
Schmitz, M., Greis, C., Ottis, P., Silva, C.J., Schulz-Schaeffer, W.J., Wrede, A., Koppe, K., Onisko, B., Requena, J.R., Govindarajan, N., Korth, C., Fischer, A., Zerr, I., 2014b. Loss of prion protein leads to age-dependent behavioral abnormalities and changes in cytoskeletal protein expression. *Mol Neurobiol* 50**,** 923-936.
Schmitz, M., Zafar, S., Silva, C.J., Zerr, I., 2014c. Behavioral abnormalities in prion protein knockout mice and the potential relevance of PrP(C) for the cytoskeleton. *Prion* 8**,** 381-386.
Seibenhener, M.L., Wooten, M.C., 2015. Use of the open field maze to measure locomotor and anxiety-like behavior in mice. *J Vis Exp***,** e52434.
Shmerling, D., Hegyi, I., Fischer, M., Blattler, T., Brandner, S., Gotz, J., Rulicke, T., Flechsig, E., Cozzio, A., von Mering, C., Hangartner, C., Aguzzi, A., Weissmann, C., 1998. Expression of amino-terminally truncated PrP in the mouse leading to ataxia and specific cerebellar lesions. *Cell* 93**,** 203-214.
Simon, P., Dupuis, R., Costentin, J., 1994. Thigmotaxis as an index of anxiety in mice. Influence of dopaminergic transmissions. *Behav Brain Res* 61**,** 59-64.
Sparkes, R.S., Simon, M., Cohn, V.H., Fournier, R.E., Lem, J., Klisak, I., Heinzmann, C., Blatt, C., Lucero, M., Mohandas, T., et al., 1986. Assignment of the human and mouse prion protein genes to homologous chromosomes. *Proc Natl Acad Sci U S A* 83**,** 7358-7362.
Stafstrom, C.E., Carmant, L. 2015. Seizures and epilepsy: an overview for neuroscientists. In: *Cold Spring Harb Perspect Med*.
Steele, A.D., Lindquist, S., Aguzzi, A., 2007. The prion protein knockout mouse: a phenotype under challenge. *Prion* 1**,** 83-93.
Striebel, J.F., Race, B., Pathmajeyan, M., Rangel, A., Chesebro, B., 2013. Lack of influence of prion protein gene expression on kainate-induced seizures in mice: studies using congenic, coisogenic and transgenic strains. *Neuroscience* 238**,** 11-18.

Su, A.I., Wiltshire, T., Batalov, S., Lapp, H., Ching, K.A., Block, D., Zhang, J., Soden, R., Hayakawa, M., Kreiman, G., Cooke, M.P., Walker, J.R., Hogenesch, J.B., 2004. A gene atlas of the mouse and human protein-encoding transcriptomes. *Proc Natl Acad Sci U S A* 101**,** 6062-6067.

Teller, S., Tahirbegi, I.B., Mir, M., Samitier, J., Soriano, J., 2015. Magnetite-amyloid-beta deteriorates activity and functional organization in an in vitro model for Alzheimer's disease. *Sci Rep* 5**,** 17261.

Urrea, L., Segura-Feliu, M., Masuda-Suzukake, M., Hervera, A., Pedraz, L., Garcia Aznar, J.M., Vila, M., Samitier, J., Torrents, E., Ferrer, I., Gavin, R., Hagesawa, M., Del Rio, J.A., 2018. Involvement of cellular prion protein in alpha-synuclein transport in neurons. *Mol Neurobiol* 55**,** 1847-1860.

Vergara, C., Ordonez-Gutierrez, L., Wandosell, F., Ferrer, I., del Rio, J.A., Gavin, R., 2015. Role of PrP(C) expression in tau protein levels and phosphorylation in Alzheimer's disease evolution. *Mol Neurobiol* 51**,** 1206-1220.

Walz, R., Amaral, O.B., Rockenbach, I.C., Roesler, R., Izquierdo, I., Cavalheiro, E.A., Martins, V.R., Brentani, R.R., 1999. Increased sensitivity to seizures in mice lacking cellular prion protein. *Epilepsia* 40**,** 1679-1682.

Watt, N.T., Taylor, D.R., Kerrigan, T.L., Griffiths, H.H., Rushworth, J.V., Whitehouse, I.J., Hooper, N.M., 2012. Prion protein facilitates uptake of zinc into neuronal cells. *Nat Commun* 3**,** 1134.

Watts, J.C., Bourkas, M.E.C., Arshad, H., 2018. The function of the cellular prion protein in health and disease. *Acta Neuropathol* 135**,** 159-178.

Wulf, M.A., Senatore, A., Aguzzi, A., 2017. The biological function of the cellular prion protein: an update. *BMC Biol* 15**,** 34.

You, H., Tsutsui, S., Hameed, S., Kannanayakal, T.J., Chen, L., Xia, P., Engbers, J.D., Lipton, S.A., Stys, P.K., Zamponi, G.W., 2012. Abeta neurotoxicity depends on interactions between copper ions, prion protein, and N-methyl-D-aspartate receptors. *Proc Natl Acad Sci U S A* 109**,** 1737-1742.

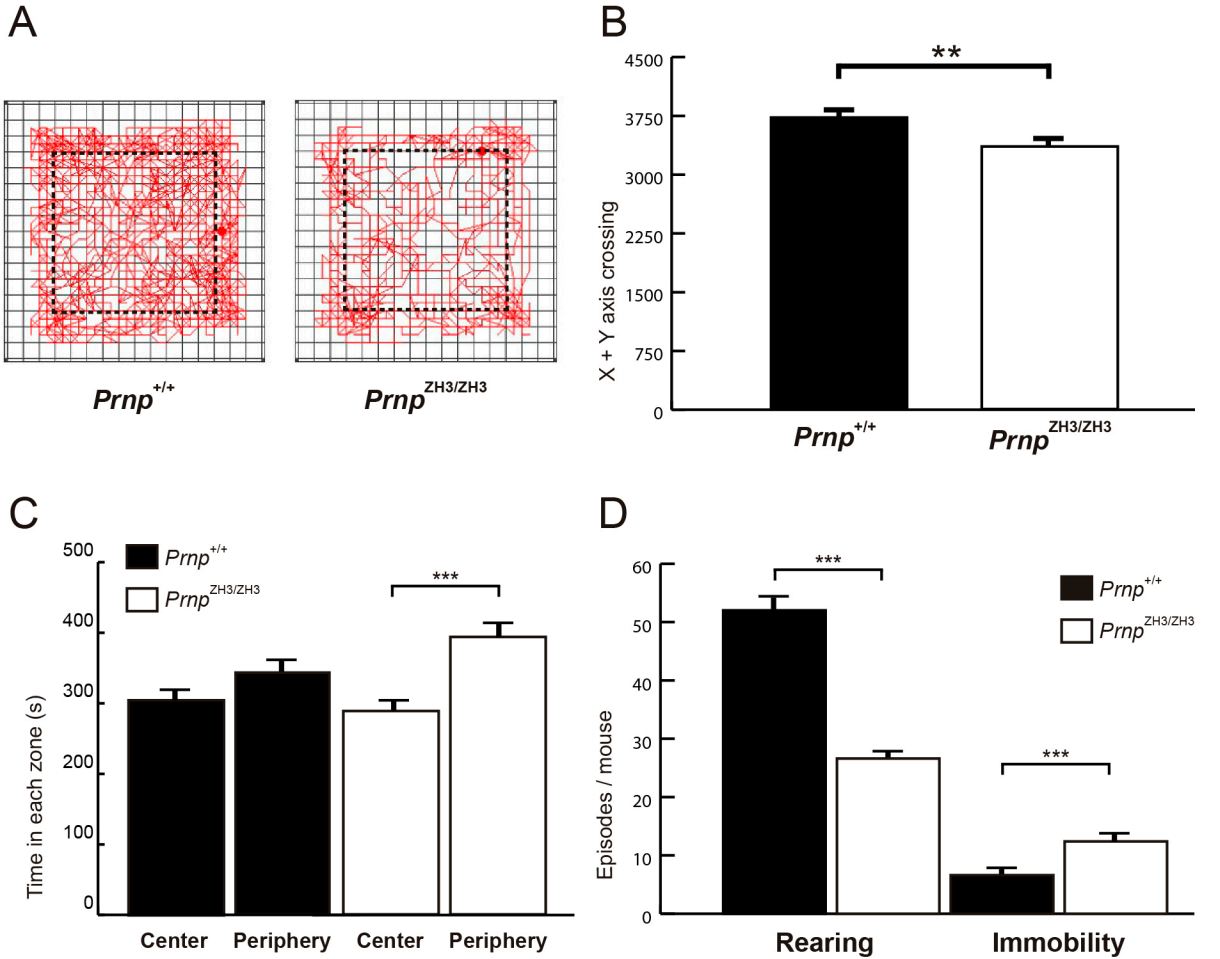
A
Prnp+/+
Prnp ZH3/ZH3
B
**
4500
3750
3000
2250
1500
750
0
X + Y axis crossing
Prnp+/+
Prnp ZH3/ZH3
C
Prnp+/+
Prnp ZH3/ZH3
***
500
400
300
200
100
0
Time in each zone (s)
Center
Periphery
Center
Periphery
D
***
***
Prnp+/+
Prnp ZH3/ZH3
60
50
40
30
20
10
0
Episodes / mouse
Rearing
Immobility

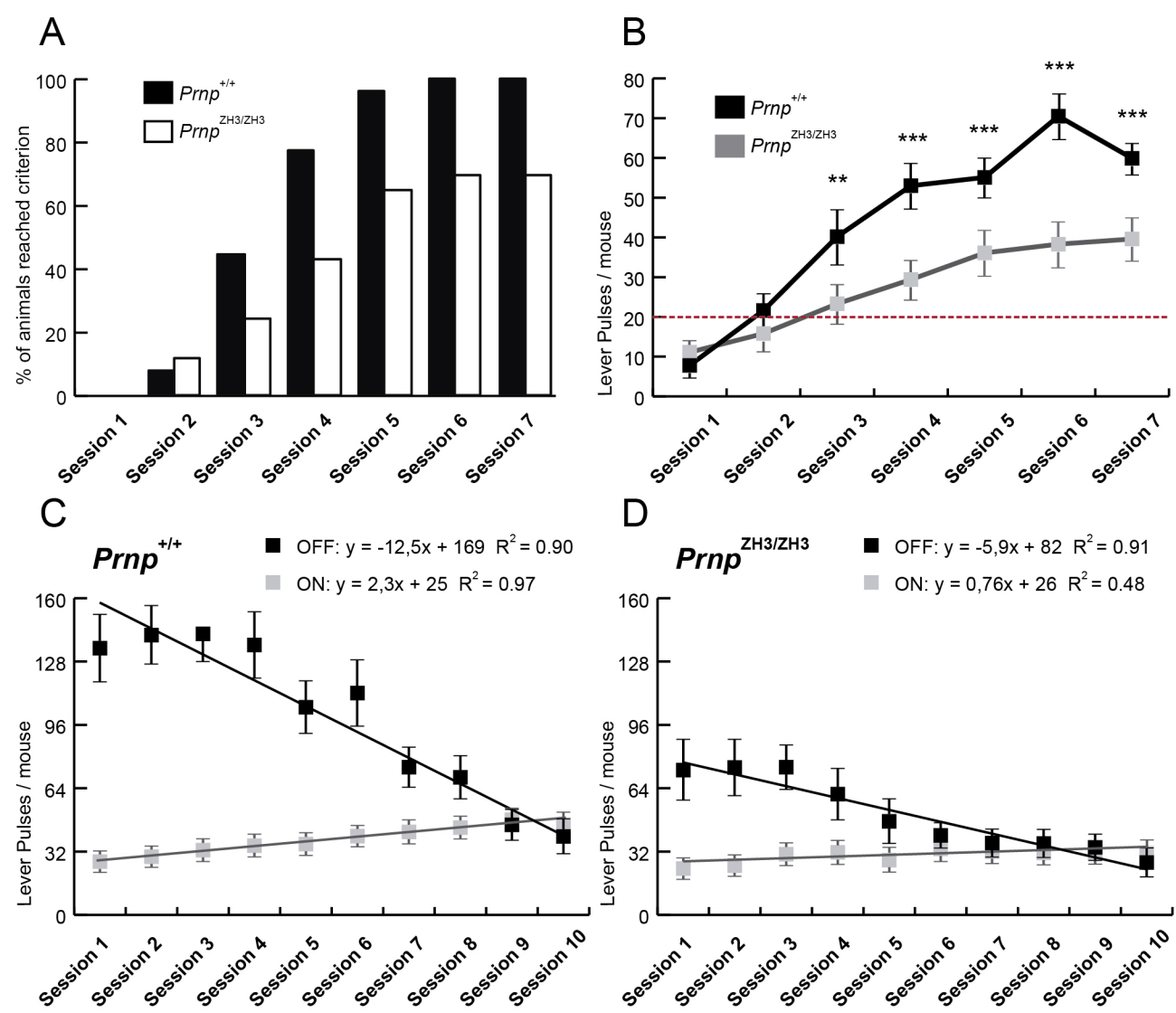
A
Prnp+/+
PrnpZH3/ZH3
% of animals reached criterion
0
20
40
60
80
100
Session 1
Session 2
Session 3
Session 4
Session 5
Session 6
Session 7
B
Prnp+/+
PrnpZH3/ZH3
Lever Pulses / mouse
0
10
20
30
40
50
60
70
80
**
***
***
***
***
Session 1
Session 2
Session 3
Session 4
Session 5
Session 6
Session 7
C
Prnp+/+
OFF: y = -12,5x + 169 R2 = 0.90
ON: y = 2,3x + 25 R2 = 0.97
Lever Pulses / mouse
0
32
64
96
128
160
Session 1
Session 2
Session 3
Session 4
Session 5
Session 6
Session 7
Session 8
Session 9
Session 10
D
PrnpZH3/ZH3
OFF: y = -5,9x + 82 R2 = 0.91
ON: y = 0,76x + 26 R2 = 0.48
Lever Pulses / mouse
0
32
64
96
128
160
Session 1
Session 2
Session 3
Session 4
Session 5
Session 6
Session 7
Session 8
Session 9
Session 10

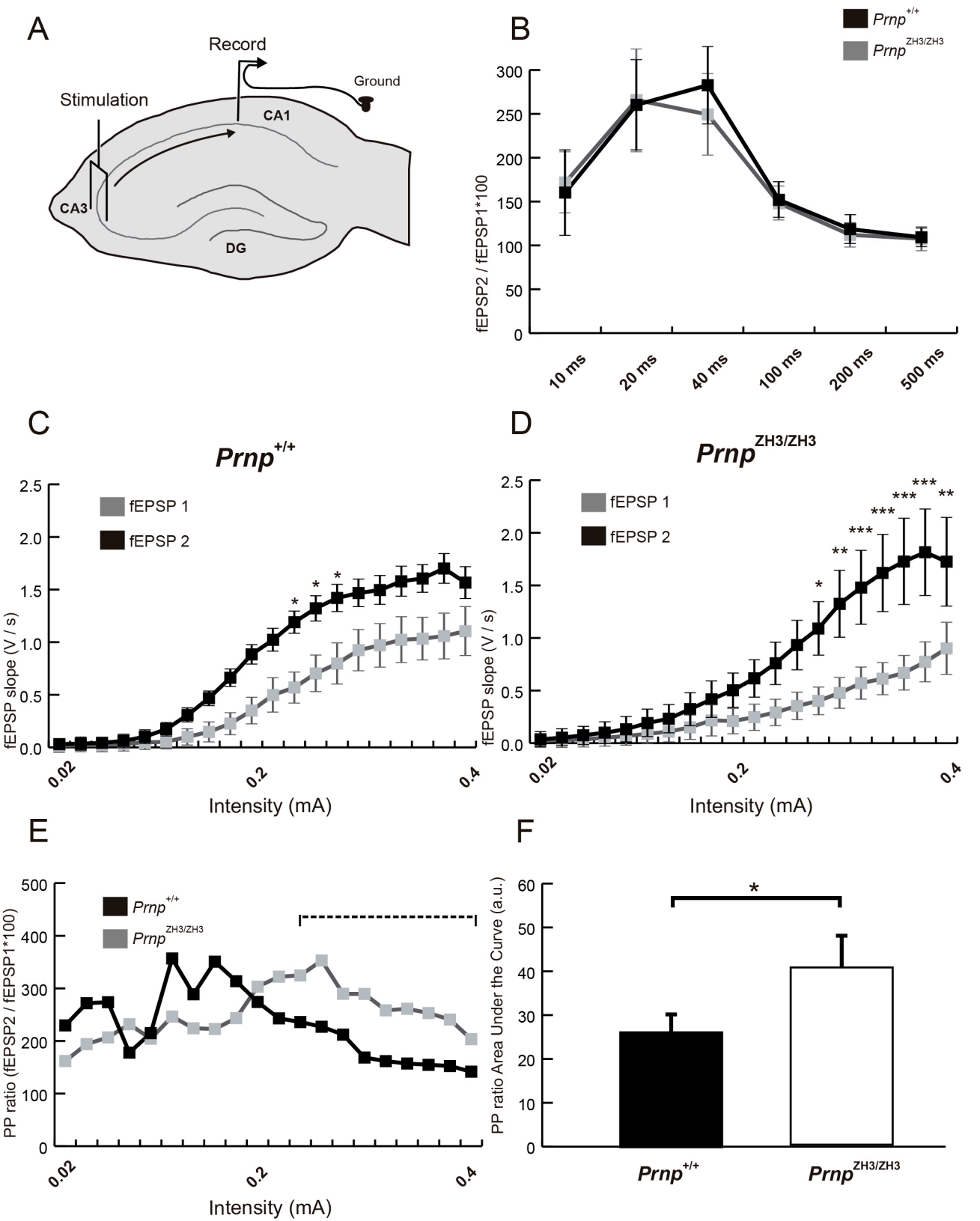
A
Record
Ground
Stimulation
CA1
CA3
DG
B
Prnp+/+
PrnpZH3/ZH3
fEPSP2 / fEPSP1*100
300
250
200
150
100
50
0
10 ms
20 ms
40 ms
100 ms
200 ms
500 ms
C
Prnp+/+
fEPSP 1
fEPSP 2
fEPSP slope (V / s)
2.5
2.0
1.5
1.0
0.5
0.0
0.02
0.2
0.4
Intensity (mA)
D
PrnpZH3/ZH3
fEPSP 1
fEPSP 2
fEPSP slope (V / s)
Intensity (mA)
E
Prnp+/+
PrnpZH3/ZH3
PP ratio (fEPSP2 / fEPSP1*100)
500
400
300
200
100
0
0.02
0.2
0.4
Intensity (mA)
F
PP ratio Area Under the Curve (a.u.)
60
50
40
30
20
10
0
*
Prnp+/+
PrnpZH3/ZH3

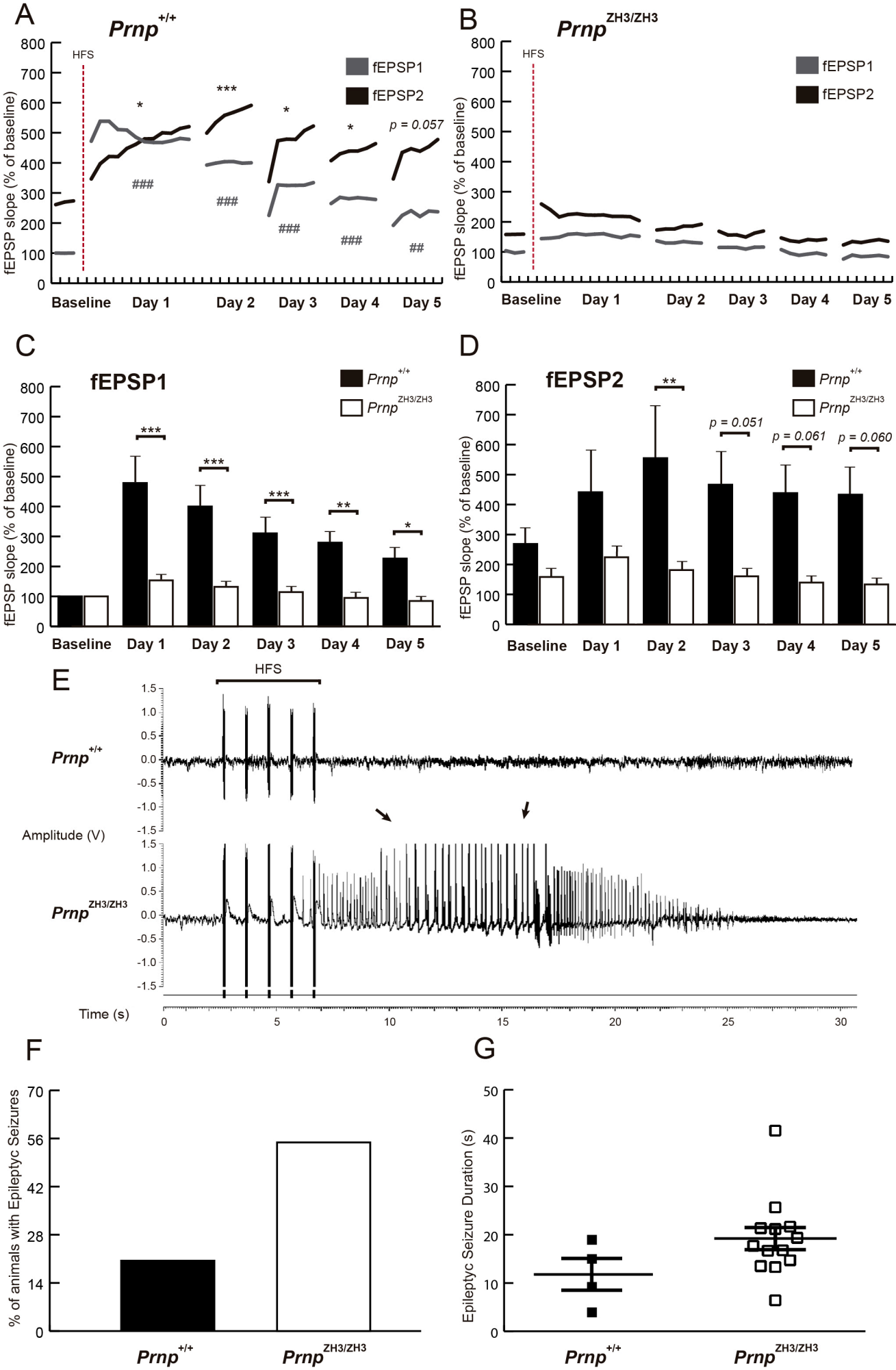
A
Prnp+/+
HFS
fEPSP1
fEPSP2
fEPSP slope (% of baseline)
p = 0.057
Baseline
Day 1
Day 2
Day 3
Day 4
Day 5
B
Prnp ZH3/ZH3
C
fEPSP1
D
fEPSP2
p = 0.051
p = 0.061
p = 0.060
E
Amplitude (V)
Time (s)
F
% of animals with Epileptyc Seizures
G
Epileptyc Seizure Duration (s)

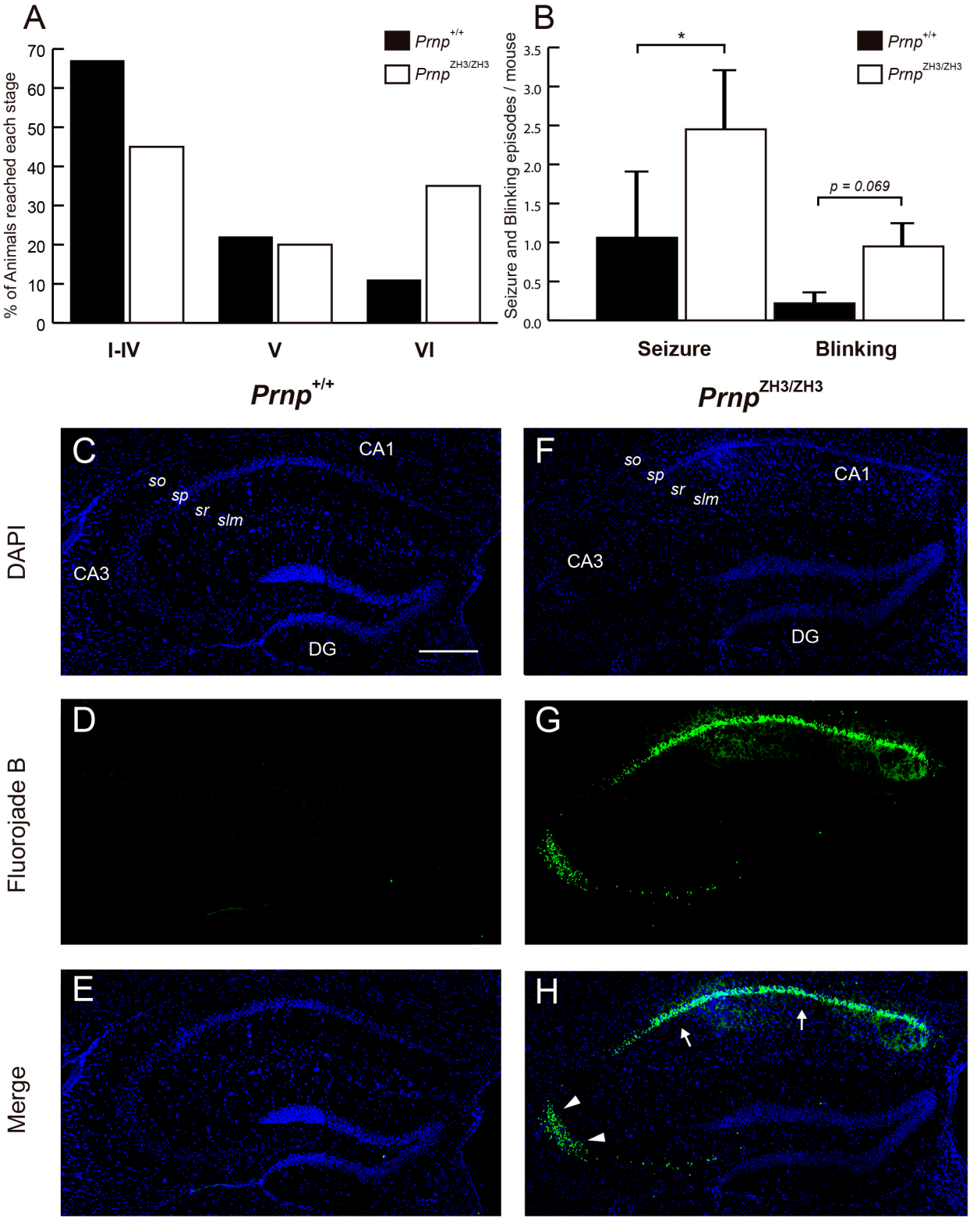
A
% of Animals reached each stage
70
60
50
40
30
20
10
0
Prnp+/+
PrnpZH3/ZH3
I-IV
V
VI
B
Seizure and Blinking episodes / mouse
3.5
3.0
2.5
2.0
1.5
1.0
0.5
0.0
*
p = 0.069
Seizure
Blinking
Prnp+/+
PrnpZH3/ZH3
DAPI
Fluorojade B
Merge
C
CA1
so
sp
sr
slm
CA3
DG
F
so
sp
sr
slm
CA1
CA3
DG
D
G
E
H

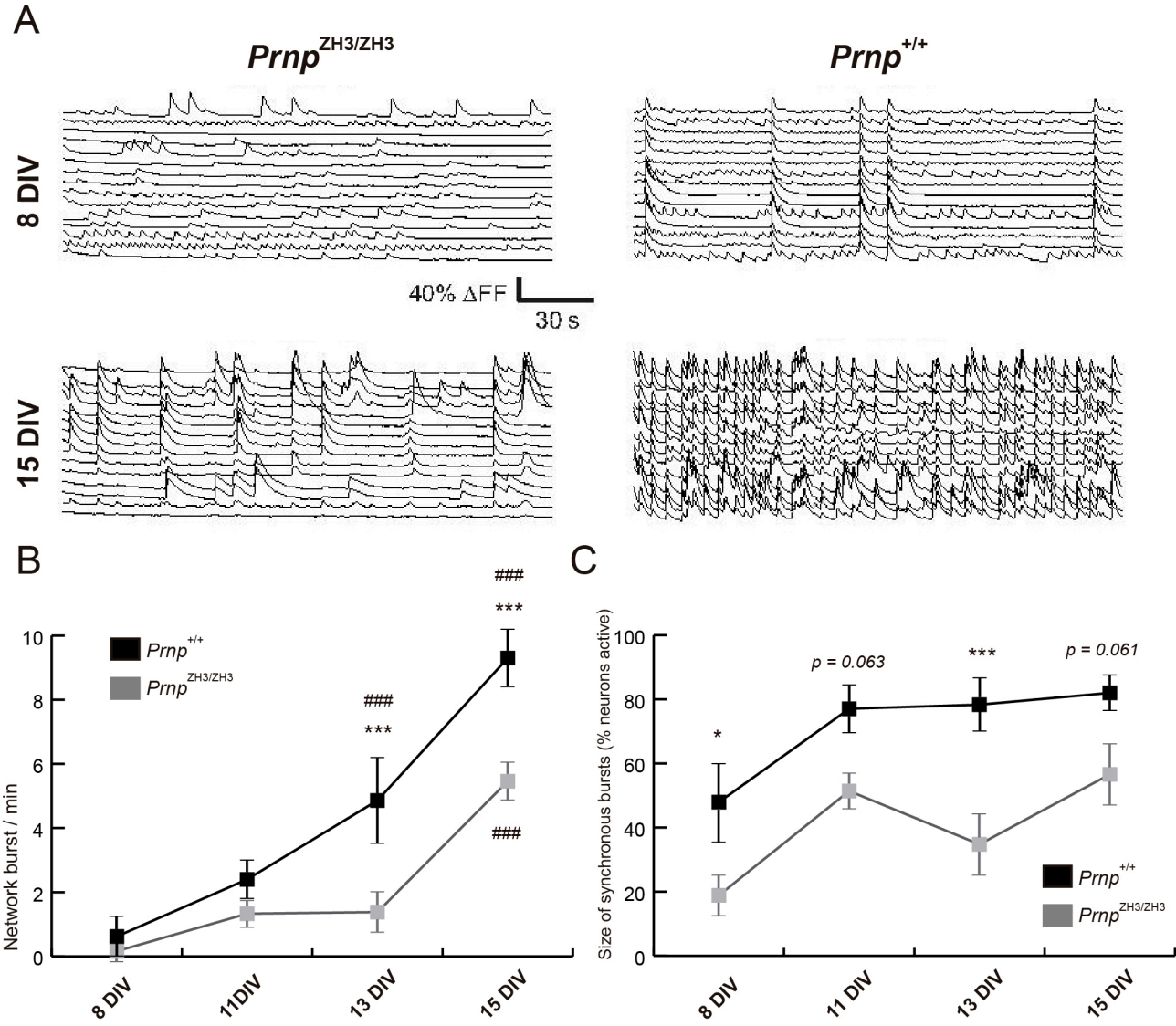
A
Prnp ZH3/ZH3
Prnp +/+
8 DIV
15 DIV
40% ΔFF
30 s
B
Prnp +/+
Prnp ZH3/ZH3
Network burst / min
8 DIV
11DIV
13 DIV
15 DIV
###
***
C
Size of synchronous bursts (% neurons active)
p = 0.063
p = 0.061
*
***
8 DIV
11 DIV
13 DIV
15 DIV

A

***Prnp*$^{+/+}$** ***Prnp*$^{ZH3/ZH3}$**

B

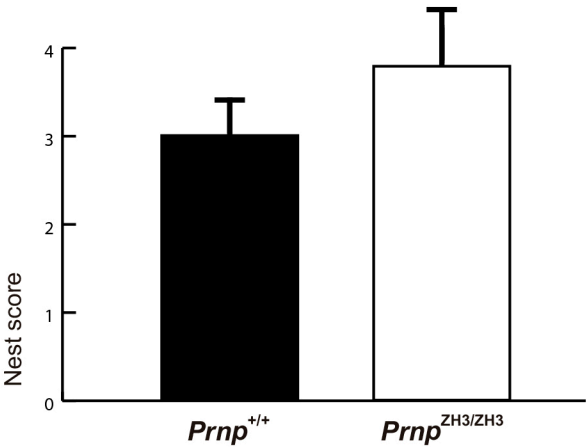

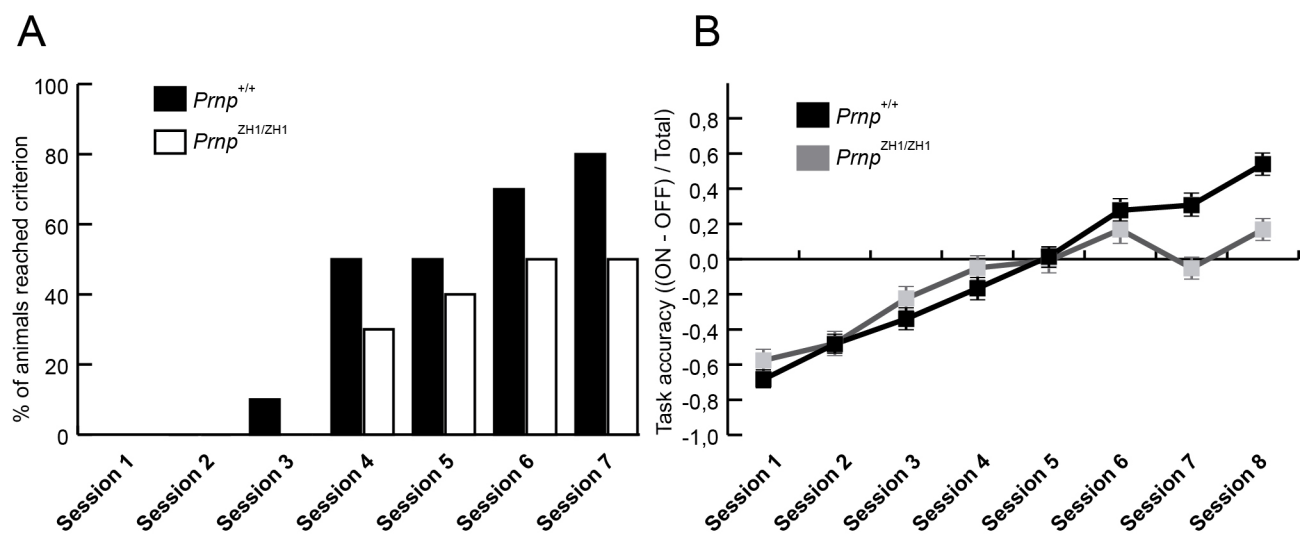
A
B
Prnp+/+
PrnpZH1/ZH1
% of animals reached criterion
100
80
60
40
20
0
Session 1
Session 2
Session 3
Session 4
Session 5
Session 6
Session 7
Task accuracy ((ON - OFF) / Total)
0,8
0,6
0,4
0,2
0,0
-0,2
-0,4
-0,6
-0,8
-1,0
Session 8

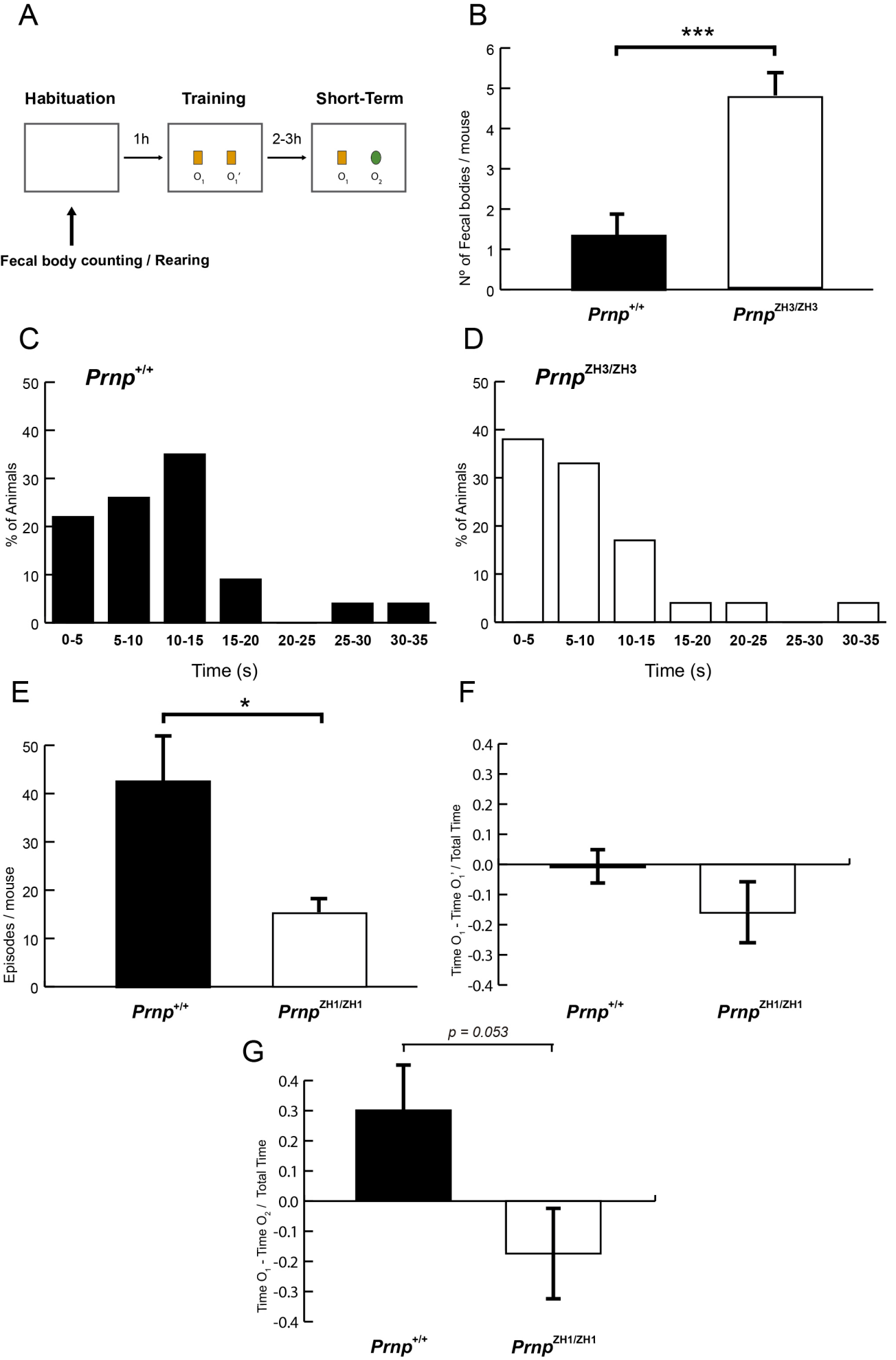
A
Habituation
Training
Short-Term
1h
2-3h
O1
O1'
O1
O2
Fecal body counting / Rearing
B
***
Nº of Fecal bodies / mouse
0
1
2
3
4
5
6
Prnp+/+
PrnpZH3/ZH3
C
Prnp+/+
% of Animals
0
10
20
30
40
50
0-5
5-10
10-15
15-20
20-25
25-30
30-35
Time (s)
D
PrnpZH3/ZH3
% of Animals
0
10
20
30
40
50
0-5
5-10
10-15
15-20
20-25
25-30
30-35
Time (s)
E
*
Episodes / mouse
0
10
20
30
40
50
Prnp+/+
PrnpZH1/ZH1
F
Time O1 - Time O1' / Total Time
-0.4
-0.3
-0.2
-0.1
0.0
0.1
0.2
0.3
0.4
Prnp+/+
PrnpZH1/ZH1
G
p = 0.053
Time O1 - Time O2 / Total Time
-0.4
-0.3
-0.2
-0.1
0.0
0.1
0.2
0.3
0.4
Prnp+/+
PrnpZH1/ZH1

A

Downregulated genes

Description	GeneRatio	p adjust
Neuronal System	40/405	6.61E-06
Protein-protein interactions at synapses	16/405	9.29E-06
Processing of Capped Intron-Containing Pre-mRNA	27/405	0.002247556
Neurotransmitter receptors and postsynaptic signal transmission	17/405	0.021385061
mRNA Splicing	20/405	0.026226473
Transmission across Chemical Synapses	20/405	0.042856307

Upregulated genes
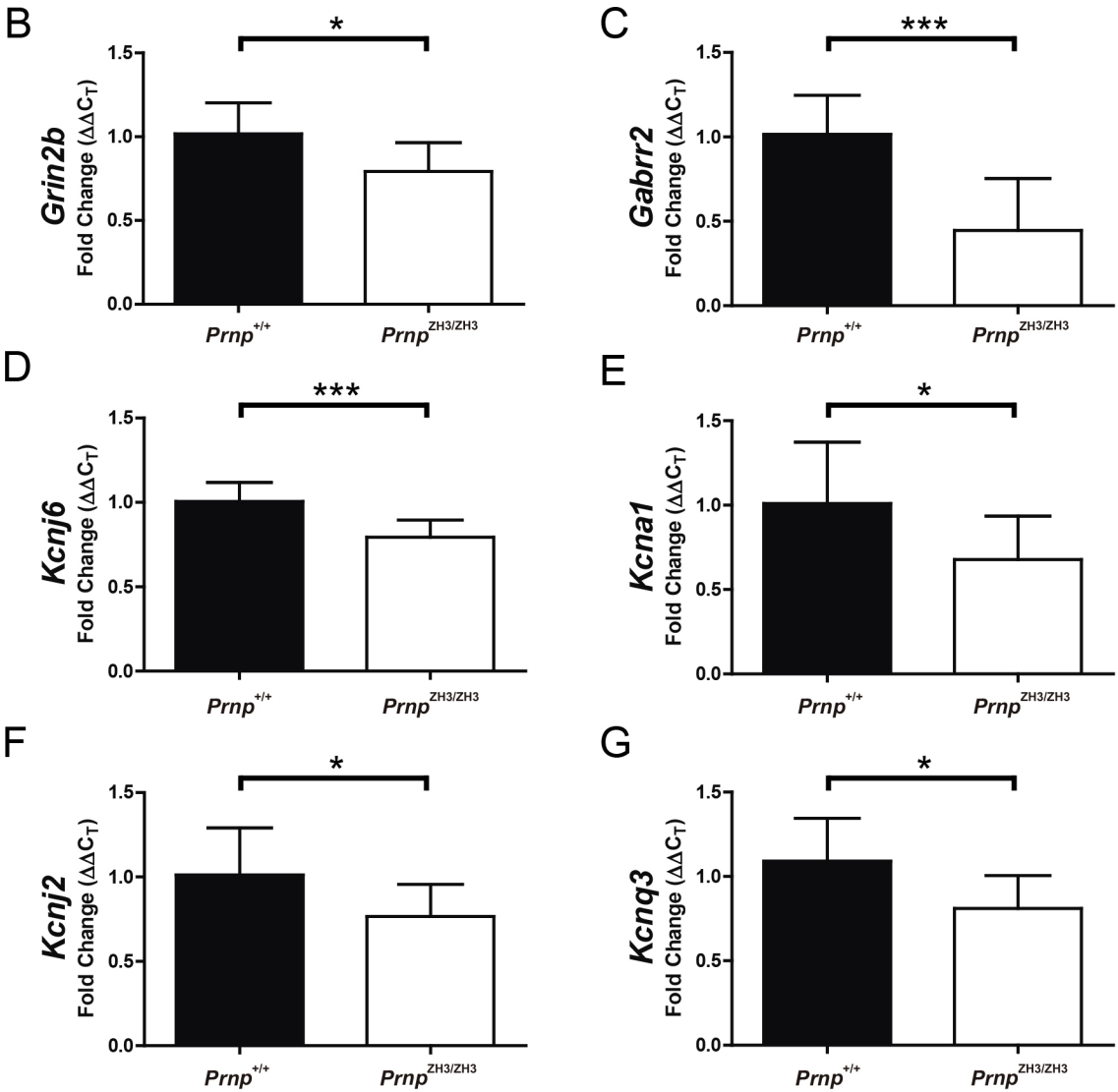
Description	GeneRatio	p adjust
The citric acid (TCA) cycle and respiratory electron transport	19/398	0.019694864
Translation	22/398	0.032052466